Space for WHAM: a multi-region, multi-stock generalization of the Woods Hole Assessment Model with an application to black sea bass

Timothy J. Miller[1] Kierstin Curti Alexander C. Hansell

21 January, 2025

[1]timothy.j.miller@noaa.gov, Northeast Fisheries Science Center, National Marine Fisheries Service, 166 Water Street, Woods Hole, MA 02543, USA

Main Message

Describes the multi-region, multi-stock generalization of WHAM and its usage to evaluate evidence of alternative hypotheses about temperature effects on recruitment of black sea bass stock components.

Abstract

The Woods Hole Assessment Model is a state-space age-structured assessment model that is used to assess and manage many stocks in the Northeast US. We first describe a multi-stock, multi-region extension of WHAM that treats the population and fleet dynamics seasonally and allows movement by season and region to be functions of time and age-varying autocorrelated random effects and environmental covariates. We then illustrate the model by applying it to data for the northern and southern components of the Northeast United States black sea bass stock and evaluate alternative hypotheses of bottom temperature and random effects on recruitment and natural mortality. We show strong evidence for temperature effects on recruitment, primarily for the northern stock component, and no evidence for including random effects or temperature effects on age 1 natural mortality.

Introduction

A state-space statistical approach and maximum marginal likelihood or Bayesian fitting of stock assessment models allows estimation of time and age-varying population attributes as random effects (Nielsen and Berg 2014; Cadigan 2016; Miller et al. 2016b). This estimation approach is considered an essential feature of gold-standard assessment models that we use in tactical management of commercially important fish stocks (Punt et al. 2020). The State-space Assessment Model (SAM, Nielsen and Berg 2014) continues to be developed and remains widely used within the International Council for the Exploration of the Sea (ICES) to assess European fish stocks. Various state-space models are being used to manage cod and plaice stocks in the waters of Eastern Canada (Perreault et al. 2020; Varkey et al. 2022) and to the south, the Woods Hole Assessment Model (WHAM, Miller and Stock 2020; Stock and Miller 2021) is now used to assess many fish stocks in the Northwest Atlantic Ocean (NEFSC 2022a, 2022b; NEFSC 2024).

WHAM is an R package developed and maintained at NOAA's Northeast Fisheries Science Center [https://timjmiller.github.io/wham]. WHAM can be configured to fit a wide range of age-structured models from traditional statistical catch-at-age models without any random effects to models with several time and age varying process errors and effects of environmental covariates on various population parameters. Like SAM, WHAM models are built using the Template Model Builder package (TMB, Kristensen et al. 2016) which provides a computationally efficient means of fitting an extremely wide class of models with random effects. WHAM has undergone active development since its creation and includes random effects options for recruitment, inter-annual transitions of numbers at age (hereafter referred to as "survival"), fishery and index selectivity, natural mortality, and catchability.

However, WHAM has only allowed one stock (component) and a single region and without seasonal changes in stock dynamics. Using such models for stocks that have subcomponents with varying seasonal movement can provide incorrect inferences and poor management advice (Ying et al. 2011; Cao et al. 2014; Bosley et al. 2022). Furthermore, the ability to account for spatial structure and model multiple stocks are also important features of leading-edge assessment modeling frameworks (Punt et al. 2020). We describe here the implementation of these features and other extensions since Stock and Miller (2021) in WHAM version 2.0. Many of these new configuration options can also be useful when modeling a single stock and region.

We developed this extension of WHAM in concert with a research track assessment process for black sea bass (*Centropristis striata*) (NEFSC 2023). Previous black sea bass assessments assumed two stock components (North and South), each assessed with a separate statistical catch at age assessment. The stock was split into two regions to account for spatial dynamics and improve model diagnostics (ASMFC 2016). Additionally,

black sea bass have complex spatial dynamics and make seasonal migrations, moving inshore in the spring and offshore in the fall (Moser and Shepherd 2009). Black sea bass distribution has been linked to warming waters on the northwest shelf (Bell et al. 2015) and it is hypothesized that black sea bass are especially susceptible to climate change with likely increases in distribution and productivity due to warming water temperatures (Hare 2016). Thus, a focus of the research track assessment was to develop an assessment platform that could capture multiple stock components, complex seasonal movement and explore environmental drivers of population dynamics (NEFSC 2023).To illustrate the usage of WHAM 2.0 we apply it to two stock components of black sea bass off the coast of the NEUS using most of the model assumptions that were accepted during the peer-review process. However, here we evaluate evidence for alternative hypotheses of temporal variation and effects specifically of bottom temperature on recruitment and natural mortality of age 1 individuals.

When modeling multiple stock components occurring in different regions further dimensionality is added to the class of possible equilbrium reference points (e.g., Kapur et al. 2021). Short term projections are also an important part of the management process and the separation of observation and process errors in state-space models allows uncertainty in projected attributes such as recruitment and spawning stock biomass (SSB) without external simulation exercises. Finally, the inclusion of explicit effects of environmental covariates in the model also requires some assumptions on how they are treated in projections and reference points. We demonstrate some of options of WHAM version 2.0 provide biological reference points and short-term projections.

Methods

WHAM description

Many of the options and equations of WHAM version 2.0 are the same as those in Stock and Miller (2021), so we will only describe extensions and differences that have occurred since their first description of WHAM. The new version of WHAM can model multiple stocks each with their own movement, harvest, and natural mortality. Much of the description below is for a specific stock s, but, for simplicity, this subscript is implicit except when necessary.

The probability transition matrix

Because individuals may be alive in one of several regions or harvested in one of several fleets, it is helpful to consider these as distinct categories or states and treat the number of individuals occurring in each category over time as a multi-state model. Approaches to modeling transitions among these states may treat time discretely (e.g., Arnason 1972; Schwarz et al. 1993) or continuously (e.g., Hearn et al. 1987; Commenges 1999; Andersen and Keiding 2002). Multi-state models can define a probability transition matrix (PTM) that describes the probability of individuals occurring in different states at the end of a time interval δ, conditional on being in each of those state at beginning of the interval. For fish populations, these states would be defined as being alive in a particular region or deceased due to fishing from a particular fleet or natural mortality. The time interval i with duration δ_i would be a season and the PTMs would be uniquely defined for each stock by season i, year y, and age a on January 1. Each row and column of the PTM correspond to one the states: alive in region r, dead in fleet f, or dead from natural causes. The probabilities in each row sum to unity and assume an individual is in the corresponding state at the beginning of the interval. Given n_R regions and n_F fleets, the square PTM ($n_R + n_F + 1$ rows and columns) as a function of sub-matrices is

$$\mathbf{P}_{y,a,i} = \begin{bmatrix} \mathbf{O}_{y,a,i} & \mathbf{H}_{y,a,i} & \mathbf{D}_{y,a,i} \\ 0 & \mathbf{I}_H & 0 \\ 0 & 0 & 1 \end{bmatrix} \tag{1}$$

where

$$\mathbf{O}_{y,a,i} = \begin{bmatrix} O_{y,a,i}(1,1) & \cdots & O_{y,a,i}(1,n_R) \\ \vdots & \ddots & \vdots \\ O_{y,a,i}(n_R,1) & \cdots & O_{y,a,i}(n_R,n_R) \end{bmatrix}$$

is the $n_R \times n_R$ matrix defining survival and occurring in each region at the end of the interval,

$$\mathbf{H}_{y,a,i} = \begin{bmatrix} H_{y,a,i}(1,1) & \cdots & H_{y,a,i}(1,n_F) \\ \vdots & \ddots & \vdots \\ H_{y,a,i}(n_R,1) & \cdots & H_{y,a,i}(n_R,n_F) \end{bmatrix}$$

is the $n_R \times n_F$ matrix defining probabilities of being captured in each fleet during the interval, and $\mathbf{D}_{y,a,i}$ is the $n_R x 1$ matrix of probabilities of dying due to natural mortality during the interval. We have the identity matrix $\mathbf{I}_H$ for the states for capture by each fleet and a 1 for the state for natural mortality because the probabilities of being in one of the mortality states given starting the interval in that state is unity (no

zombies allowed).

WHAM uses these PTMs to model abundance proportions in each state rather than true probabilities where numbers in each state would be multinomial distributed as in a model for tagging data where fates of individual fish are assumed independent. The PTMs determine the expected numbers 1) in each state on January 1 of year $t+1$ at age $a+1$ given the abundances at age a on January 1 of year t, 2) captured over the year in each fleet, 3) available to each index, and 4) alive at the time and in the region where spawning occurs.

Single region PTMs

When there is only one region,

$$\mathbf{P}_{y,a,i} = \begin{bmatrix} S_{y,a,i} & \mathbf{H}_{y,a,i} & D_{y,a,i} \\ 0 & \mathbf{I}_H & 0 \\ 0 & 0 & 1 \end{bmatrix} \tag{2}$$

where $S_{y,a,i} = e^{-Z_{y,a,i}\delta_i}$, $\mathbf{H}_{y,a,i}$ is a 1 x n_F matrix with elements for each fleet f: $\frac{F_{y,a,i,f}}{Z_{y,a,i}}\left(1 - e^{-Z_{y,a,i}\delta_i}\right)$, $D_{y,a,i} = \frac{M_{y,a}}{Z_{y,a,i}}\left(1 - e^{-Z_{y,a,i}\delta_i}\right)$, and $Z_{y,a,i} = M_{y,a} + \sum_{f=1}^{n_F} F_{y,a,i,f}$ is the total mortality rate.

Multi-region PTMs

When there is more than one region, WHAM can model survival and movement as processes occurring sequentially or simultaneously. The sequential assumption is used widely in spatially explicit model (e.g., Stock Synthesis, Methot and Wetzel 2013). Under the sequential assumption, survival and death occur over the interval and movement among regions occurs instantly at either the beginning or the end of the interval. WHAM is configured to have movement occur after survival and mortality:

$$\mathbf{O}_{y,a,i} = \mathbf{S}_{y,a,i}\boldsymbol{\mu}_{y,a,i}$$

where $\mathbf{S}_{y,a,i}$ is a $n_R \times n_R$ diagonal matrix of proportions surviving in each region (given they start in that region)

$$\mathbf{S}_{y,a,i} = \begin{bmatrix} e^{-Z_{y,a,i,1}\delta_i} & 0 & \cdots & 0 \\ 0 & e^{-Z_{y,a,i,2}\delta_i} & \cdots & 0 \\ \vdots & \vdots & \ddots & \vdots \\ 0 & \cdots & 0 & e^{-Z_{y,a,i,n_R}\delta_i} \end{bmatrix}$$

and $\boldsymbol{\mu}_{y,a,i}$ is a $n_R \times n_R$ matrix of probabilities of moving from one region to another or staying in the region they occurred at the beginning of the interval:

$$\boldsymbol{\mu}_{y,a,i} = \begin{bmatrix} 1 - \sum_{r' \neq 1} \mu_{1 \to r',y,a,i} & \mu_{1 \to 2,y,a,i} & \cdots & \mu_{1 \to R,y,a,i} \\ \mu_{2 \to 1,y,a,i} & 1 - \sum_{r' \neq 2} \mu_{2 \to r',y,a,i} & \cdots & \mu_{2 \to R,y,a,i} \\ \vdots & \vdots & \ddots & \vdots \\ \mu_{R \to 1,y,a,i} & \cdots & \mu_{R \to R-1,y,a,i} & 1 - \sum_{r' \neq R} \mu_{R \to r',y,a,i} \end{bmatrix}$$

WHAM assumes each fleet f can harvest in only one region (r_f) during specified seasons. So, for each fleet f, row r_f and column f of $\mathbf{H}_{y,a,i}$ will be $F_{y,a,i,f} \left(1 - e^{-Z_{y,a,i,r}\delta_i}\right) / Z_{y,a,i,r}$ when fleet f is harvesting during the interval δ_i and all other elements will be zero. Row r of the single-column matrix $\mathbf{D}_{y,a,i}$ is $M_{y,a,r} \left(1 - e^{-Z_{y,a,i,r}\delta_i}\right) / Z_{y,a,i,r}$

When survival and movement are assumed to occur simultaneously, all movement and mortality parameters are instantaneous rates. We obtain the probability transition matrix over an interval δ_i by exponentiating the instantaneous rate matrix (Miller and Andersen 2008)

$$\mathbf{P}_{y,a,i} = e^{\mathbf{A}_{y,a,i}\delta_i}$$

The instantaneous rate matrix takes rates of movement between regions and the mortality rates for each fleet and region. Along the diagonal is the negative of the sum of the other rates (the hazard) so each row sums to zero. For two regions and one fleet operating in each region:

$$\mathbf{A}_{y,a,i} = \begin{bmatrix} a_{y,a,i,1} & \mu_{1 \to 2,y,a,i} & F_{y,a,i,1} & 0 & M_{y,a,1} \\ \mu_{2 \to 1,y,a,i} & a_{y,a,i,2} & 0 & F_{y,a,i,2} & M_{y,a,2} \\ 0 & 0 & 0 & 0 & 0 \\ 0 & 0 & 0 & 0 & 0 \\ 0 & 0 & 0 & 0 & 0 \end{bmatrix}.$$

where $a_{y,a,i,r} = -(\mu_{r \to r',y,a,i} + F_{y,a,i,r_f} + M_{y,a,r})$. When there is one region, n_f fleets, and $\delta_i = 1$, exponentiating the instantaneous rate matrix results in the PTM defined in Eq. 2.

Seasonality

Seasonality can be configured to accommodate characteristics of spawning, movement, and fleet-specific behavior. The annual time step can be divided into K (any number) seasons and the interval size δ_i for each season i does not need to be equal to any other seasonal interval. Under the Markov assumption, the PTM of surviving and moving and dying over K intervals $\delta_1, \ldots, \delta_K$ (i.e., the entire year) is just the product of the PTMs for each interval:

$$\mathbf{P}_{y,a}(\delta_1, \ldots, \delta_K) = \prod_{i=1}^{K} \mathbf{P}_{y,a,i}(\delta_i).$$

For a stock spawning at some fraction of the year $0 < t_s < 1$ in interval δ_j, the fraction of time in season j is

$$\delta_{s,j} = t_s - \sum_{i=0}^{j-1} \delta_i$$

and the PTM defining the proportions in each state at time t_s for age a is

$$\mathbf{P}_{y,a}\left(\delta_1, \ldots, \delta_{j-1}, \delta_{s,j}\right) = \mathbf{P}_{y,a}\left(t_s\right) = \left[\prod_{i=1}^{j-1} \mathbf{P}_{y,a,i}(\delta_i)\right] \mathbf{P}_{y,a,j}(\delta_{s,j}). \tag{3}$$

Similarly, for an index m occurring at fraction of the year t_m in interval δ_j the proportions in each state at the time of the observation is

$$\mathbf{P}_{y,a}\left(\delta_1, \ldots, \delta_{j-1}, \delta_{m,j}\right) = \mathbf{P}_{y,a}\left(t_m\right) = \left[\prod_{i=1}^{j-1} \mathbf{P}_{y,a,i}(\delta_i)\right] \mathbf{P}_{y,a,j}(\delta_{m,j}). \tag{4}$$

Numbers at age

When there are n_R regions and n_F fleets, the vector of abundance in each state at age $a > 1$ on January 1 is $\mathbf{N}_{y,a} = (\mathbf{N}'_{O,y,a}, \mathbf{0}')'$ where $\mathbf{N}_{O,y,a} = (N_{y,a,1}, \ldots, N_{y,a,n_R})'$ is the number in the states corresponding to being alive in each region and $\mathbf{0}$ is a vector $(n_F + 1)$ for the numbers captured in each fleet and dead from natural mortality because no age a fish have died yet on January 1.

Each stock s is assumed to spawn and recruit in one region r_s. So for age $a = 1$, $\mathbf{N}_{O,y,1}$ is 0 except for row $r = r_s$. Options for configuring recruitment ($N_{y,1,r_s}$) for each stock are the same as previous versions of WHAM (Miller and Stock 2020). If recruitment is assumed to be a function of SSB, it is only the spawning population in region r_s at the time of spawning that constitutes the SSB in the stock-recruit function. However, models can configure spawning individuals to occur in other regions at the time of spawning. Aside from treating recruitment as a random walk, the general model for annual recruitment as random

effects is

$$\log\left(N_{y,1,r_s}\right)|\mathrm{SSB}_{y-1,r_s} = f\left(\mathrm{SSB}_{y-1,r_s}\right) + \varepsilon_{y,1,r_s}$$

where

$$\mathrm{SSB}_{s,y} = \sum_{a=1}^{A} w_{s,y,a}\mathrm{mat}_{s,y,a}\mathbf{O}_{s,y,a,r_s}(t_s)'\mathbf{N}_{O,s,y,a}$$

where $w_{s,y,a}$ is the mean weight at age of spawning individuals, $\mathrm{mat}_{s,y,a}$ is the maturity at age, and $\mathbf{O}_{s,y,a,r_s}(t_s)$, the r_s column of the upper-left submatrix of Eq. 3, are the probabilities of surviving and occurring in region r_s at time t_s given being alive in each region at the start of the year.

As in previous versions of WHAM, the transitions in numbers at age from one year to another after recruitment can be treated deterministically or as functions of random effects. The predicted numbers at age in year y at age a for a given stock are vector analogs ($\mathbf{N}_{O,y,a}$) of the equations for numbers at age in the standard WHAM model (Stock and Miller 2021). For ages $a = 2, \ldots, A-1$, where A is the plus group, the expected number alive in each region at the beginning of the following year and next age class age can be obtained from the first n_R elements of the vector

$$\mathbf{P}'_{y-1,a-1}\mathbf{N}_{y-1,a-1}.$$

The numbers alive in each region can also be modeled more simply using the sub-matrix $\mathbf{O}_{y,a}$. The general model for the transitions in abundance at age is

$$\log\left(\mathbf{N}_{O,y,a}\right)|\mathbf{N}_{O,y-1,a-1} = \log\left(\mathbf{O}'_{y-1,a-1}\mathbf{N}_{O,y-1,a-1}\right) + \boldsymbol{\varepsilon}_{y,a}$$

for ages $a = 2, \ldots, A-1$, and for the plus group

$$\log\left(\mathbf{N}_{O,y,A}\right)|\mathbf{N}_{O,y-1,a-1}, \mathbf{N}_{O,y-1,A} = \log\left(\mathbf{O}'_{y-1,A-1}\mathbf{N}_{O,y-1,A-1} + \mathbf{O}'_{y-1,A}\mathbf{N}_{O,y-1,A}\right) + \boldsymbol{\varepsilon}_{y,A}$$

where $\boldsymbol{\varepsilon}_{y,a}$ is the vector of region-specific errors for a given stock, which are independent across stocks and regions, but the same correlation structures as previous versions are possible across ages and years for a given stock and region. When there is autocorrelation with age, WHAM now assumes this applies only to ages $a > 1$ by default so that recruitment random effects are independent of those for for the annual transitions of older age classes. So the general covariance structure for a given stock at ages $a > 1$ in region r is that of

a two-dimensional first-order autoregressive (2DAR1) process

$$Cov\left(\varepsilon_{y,a,r},\varepsilon_{y',a',r}\right)=\frac{\rho_{N,\text{age},r}^{|a-a'|}\rho_{N,\text{year},r}^{|y-y'|}\sigma_{N,a,r}\sigma_{N,a',r}}{\left(1-\rho_{N,\text{age},r}^{2}\right)\left(1-\rho_{N,\text{year},r}^{2}\right)}$$

and that for age 1 is just AR1 across years

$$Cov\left(\varepsilon_{y,1},\varepsilon_{y',1}\right)=\frac{\rho_{N,1,\text{year}}^{|y-y'|}\sigma_{N,1}^{2}}{1-\rho_{N,1,\text{year}}^{2}}.$$

When the transitions in abundance at age are treated deterministically, $\boldsymbol{\varepsilon}_{y,a}=0$. Since recruitment for a given stock currently only occurs in one region r_s there is only a single time-varying recruitment random effect for each stock.

Initial numbers at age

Initial numbers at age for each stock and region can be treated as age-specific fixed effects or with an equilibrium assumption as in previous versions of WHAM. For the equilibrium option there are two parameters for each stock: the stock-specific fully-selected fishing mortality rate $\log\widetilde{F}$ and the recruitment in year 1 $\log N_{1,1,r_s}$. A stock-specific equilibrium fishing mortality at age by fleet $\tilde{F}_{a,f}$ is the product of $\widetilde{F}$ and the selectivity across fleets in the first year

$$\text{sel}_{1,a,f}=\frac{F_{1,a,f}}{\max_a\sum_{f=1}^{n_F}F_{1,a,f}}.$$

We use $\widetilde{F}_{a,f}$ to define an equilibrium abundance per recruit by region at age a conditional on recruiting to each region

$$\widetilde{\mathbf{O}}_a=\begin{cases}\prod_{j=0}^{a-1}\mathbf{O}_j & 1\le a<A\\ \left[\prod_{j=0}^{a-1}\mathbf{O}_j\right]\left(\mathbf{I}-\mathbf{O}_A\right)^{-1} & a=A\end{cases}\tag{5}$$

where $\mathbf{O}_j$ is the equilibrium probability of surviving age a and occurring in each region and $\mathbf{O}_0=\mathbf{I}$. Natural mortality and movement rates in the first year of the model are also used in Eq. 5. For the plus group $a=A$, $\left(\mathbf{I}-\mathbf{O}_A\right)^{-1}$ is a "fundamental matrix'' derived using the matrix version of the geometric series (Kemeny and Snell 1960). Recall that recruitment for stock s only occur in region r_s so, the equilibrium initial numbers at age a by region are

$$\mathbf{N}_{O,1,a}=\widetilde{\mathbf{O}}_a'\mathbf{N}_{O,1,1}.$$

The initial abundances at age can also be treated as independent or as AR1 random effects. Defining the

vector of initial abundance at age in region r as $\mathbf{N}_{O,1,r}$, the general model is

$$\log \mathbf{N}_{O,1,r} = \theta_{N_1,r} + \boldsymbol{\varepsilon}_{N_1,r}$$

where

$$Cov\left(\varepsilon_{N_1,a,r}, \varepsilon_{N_1,a',r}\right) = \frac{\rho_{N_1,r}^{|a-a'|}\sigma_{N_1,r}^2}{\left(1-\rho_{N_1,r}^2\right)}.$$

Parametizing movement

For each season, there are at most $n_R - 1$ parameters determining movement among regions given starting an the season in region r in either the sequential or simultaneous configurations. Movement parameters are estimated on a transformed scale via a link function $g(\cdot)$. If survival and movement occur simultaneously, the parameters are estimated with a log link function and if they are separable, an additive logit link function (like a multinomial regression) is used. On the transformed scale, the general model for the movement parameter from region r to r' in season i and year y for individuals of age a is a linear function of both random and environmental effects:

$$g(\mu_{r\to r',y,a,i}) = \theta_{r\to r',i} + \varepsilon_{r\to r',y,a,i} + \sum_{k=1}^{n_E} \beta_{r\to r',a,i,k} E_{k,y}.$$

The random effects $\varepsilon_{r\to r',y,a,i}$ are season-, and(or) region-to-region-specific and modeled most generally as 2DAR1 random effects with age and(or) year where the covariance is

$$Cov\left(\varepsilon_{r\to r',y,a,i}, \varepsilon_{r\to r',y',a',i}\right) = \frac{\rho_{r\to r',\text{age},i}^{|a-a'|}\rho_{r\to r',\text{year},i}^{|y-y'|}\sigma_{r\to r',i}^2}{\left(1-\rho_{r\to r',\text{age},i}^2\right)\left(1-\rho_{r\to r',\text{year},i}^2\right)}$$

similar to how WHAM models variation in survival, natural mortality, and selectivity. Effects of covariate E_k can be age-, season-, and(or) region-to-region-specific $\beta_{r\to r',a,i,k}$ and the same orthogonal polynomial options in the previous versions of WHAM for effects on recruitment and natural mortality are available.

There is currently no likelihood component for tagging data. Therefore, movement parameters would generally either need to be fixed or assumed to have some prior distribution, possibly based on external parameter estimates. We include prior distributions for the season and region-to-region specific (mean) movement parameters which are treated as random effects with the mean defined by the initial value of the fixed effect

counterpart and standard deviation

$$\gamma_{r\to r',i} \sim \mathrm{N}\left(\theta_{r\to r',i}, \sigma^2_{r\to r',i}\right).$$

When priors are used, the movement is defined instead as

$$g(\mu_{r\to r',y,a,i}) = \gamma_{r\to r',i} + \varepsilon_{r\to r',y,a,i} + \sum_{k=1}^{n_E} \beta_{r\to r',a,i,k} E_{k,y}$$

Natural mortality

Natural mortality options have been expanded since initial WHAM development. When not estimated, (mean) mortality rates may be stock-, region-, and age-specific. When random effects are used, the same 2DAR1 structure with age and year as described by Stock and Miller (2021) can be configured for a given stock and region. Any environmental covariate effects can be stock-, region-, and age-specific. So the general model for natural mortality is

$$\log M_{y,a,r} = \theta_{M,r} + \varepsilon_{M,r,y,a} + \sum_{k=1}^{n_E} \beta_{M,r,a,k} E_{k,y}.$$

The general covariance structure for random effects are modeled most generally as 2DAR1 random effect with age and(or) year where the covariance is

$$Cov\left(\varepsilon_{M,y,a,r}, \varepsilon_{M,y',a',r}\right) = \frac{\rho^{|a-a'|}_{M,\mathrm{age},r} \rho^{|y-y'|}_{M,\mathrm{year},r} \sigma^2_{M,r}}{\left(1-\rho^2_{M,\mathrm{age},r}\right)\left(1-\rho^2_{M,\mathrm{year},r}\right)}.$$

Catch observations

The log-normal distributional assumption for aggregate catch observations is the same as Stock and Miller (2021), but the predicted catch is now a function of catch from each stock starting the year in each region. For a given stock and age, the numbers captured in each fleet over the year are

$$\widehat{\mathbf{N}}_{H,s,y,a} = \mathbf{H}'_{s,y,a} \mathbf{N}_{O,s,y,a}$$

The predicted numbers caught be each fleet across stocks is

$$\widehat{\mathbf{N}}_{H,y,a} = \sum_{s=1}^{n_S} \widehat{\mathbf{N}}_{H,s,y,a}$$

and the predicted aggregate catch at age a is

$$\widehat{\mathbf{C}}_{y,a} = \text{diag}\left(\mathbf{c}_{y,a}\right)\widehat{\mathbf{N}}_{H,y,a}$$

where $\mathbf{c}_{y,a}$ is the vector of mean individual weight at age a for each fleet and the aggregate catch by fleet is

$$\widehat{\mathbf{C}}_{y} = \sum_{a=1}^{A}\widehat{\mathbf{C}}_{y,a}$$

The log-aggregate catch observations for fleet f are normally distributed

$$\log C_{y,f} \sim \text{N}\left(\log \widehat{C}_{y,f}, \sigma^2_{y,f}\right).$$

The predicted numbers caught for each fleet f (row f of $\widehat{\mathbf{N}}_{H,y,a}$) are used to make predicted age composition observations as described by Stock and Miller (2021). Since then, three additional likelihood options for age composition observations have been added: a logistic-normal with AR(1) correlation structure (Francis 2014), the alternative Dirichlet-multinomial parameterization described by Thorson et al. (2017), and the multivariate Tweedie (Thorson et al. 2023).

Index observations

For index m occurring in region r_m at fraction of the year t_m, the predicted abundance at t_m in region r_m is

$$\widehat{N}_{s,y,a,m} = \mathbf{O}_{s,y,a,r_m}(t_m)'\mathbf{N}_{O,s,y,a}$$

where $\mathbf{O}_{s,y,a,r_m}(t_m)$, the r_m column of the upper-left submatrix of Eq. 4, are the probabilities of surviving and occurring in region r_m at time t_m given being alive in each region at the start of the year. The predicted index at age is

$$\widehat{I}_{m,y,a} = q_{m,y}\text{sel}_{m,y,a}w_{m,y,a}\sum_{s=1}^{n_S}\widehat{N}_{s,y,a,m}$$

where $q_{m,y}$ is the catchability of the index in year y, $\text{sel}_{m,y,a}$ is the selectivity and $w_{m,y,a}$ is the average weight of individuals at age a if the index is quantified in biomass and $w_{m,y,a} = 1$ if the index is quantified in numbers. Predicted age composition observations are functions of $\widehat{I}_{m,y,a}$ as described by Stock and Miller (2021) and the likelihood options are the same as those for catch explained above.

Catchability of the index can also be treated as functions of normal random effects and(or) environmental

covariate effects

$$log\frac{q_{m,y}-l_m}{u_m-q_{m,y}} = \theta_{q,m} + \varepsilon_{q,m,y} + \sum_{k=1}^{n_E}\beta_{q,m,k}E_{k,y}$$

where u_m and l_m are the upper and lower bounds of catchability for index m (defaults are 0 and 1000) and the general covariance structure for the annual random effects is AR1

$$Cov\left(\varepsilon_{q,m,y},\varepsilon_{q,m,y'}\right) = \frac{\rho_{q,m}^{|y-y'|}\sigma_{q,m}^2}{1-\rho_{q,m}^2}.$$

Weight and Maturity at age

Weight and maturity at age are treated similarly to Stock and Miller (2021). Annual weight at age matrices for each fleet are used to calculate total catch and the weight at age is applied to catch numbers at age for any stocks caught by the fleet. Similarly, when indices and(or) associated age composition observations are measured in biomass, the weight at age matrices for the index are applied to predicted numbers at age of all stocks observed by the survey. Unique weight at age and maturity at age matrices are allowed for each stock to calculate spawning stock biomass.

Reference points

Currently a single F reference point $\widetilde{F}$ is estimated across stocks and regions and F by fleet and age is $\widetilde{F}_{f,a} = \widetilde{F}\text{sel}_{f,a}$. Selectivity is determined as before when there are multiple fleets where $\text{sel}_{f,a}$ is determined by averaging F at age over a user-defined set of years

$$\text{sel}_{a,f} = \frac{\overline{F}_{a,f}}{\max_a \sum_{f=1}^{n_F}\overline{F}_{a,f}}$$

The equilibrium spawning stock biomass per recruit for stock s in region r_s is defined as

$$\phi_s(\widetilde{F}) = \sum_{a=1}^{A}\widetilde{\mathbf{O}}_{s,a,r_s,\cdot}\mathbf{O}_{s,a,\cdot,r_s}(t_s)w_{s,a}m_{s,a} \tag{6}$$

where $w_{s,a}$ and $m_{s,a}$ are the mean individual weight and probability of maturity at age a, $\widetilde{\mathbf{O}}_{s,a}$ are as described in Eq. 5, and $\mathbf{O}_{s,a}(t_s)$ is the $n_R \times n_R$ upper-left sub-matrix of eq. 3 with the probabilities of surviving and occurring in each region r' at age $a+t_s$ given starting in region r at age a. The further subscripts $r_s,\cdot$ and $\cdot,r_s$ indictate row or column r_s, respectively. Using these rows and columns is required because of the assumption that spawning and recruitment only occur in region r_s.

The equilibrium spawning biomass per recruit (eq. 6) is conditional on the region of recruitment r_s. The equilibrium recruitment in each region $\widetilde{\mathbf{N}}_{s,1}$, depends on the stock dynamics. This version of WHAM currently only allows complete spawning region fidelity so that a stock only spawns and recruits in a single region. In this case, $\widetilde{\mathbf{N}}_{s,1}$ will be positive in the spawning region (r_s) and zero elsewhere. Similarly, the row r_s of $\mathbf{O}_s$ will be zero off of the diagonal. The matrices of probabilities of surviving and occurring in each region, $\widetilde{\mathbf{O}}_{s,a}$ and $\mathbf{O}_{s,a}(\delta_s)$, are functions of the fishing mortality rates for fleets in each region $\widetilde{F}_{f,a}$.

The matrix equilibrium yield per recruit as a function of $\widetilde{F}$ is calculated as

$$\widetilde{Y}_s(\widetilde{F}) = \sum_{a=1}^{A} \widetilde{\mathbf{O}}_{s,a,r_s,\cdot} \mathbf{H}_{s,a} \mathbf{c}_{s,a} \tag{7}$$

where $\mathbf{c}_a$ is the vector of mean individual weight at age for each fleet, and $\mathbf{H}_{s,a}$ is the submatrix of the probabilities of being captured in each fleet over the interval from a to $a+1$, defined in eq. 1.

As in previous versions of WHAM package, "static'' reference points, typically meant to be defined for prevailing conditions, average all of the inputs to the spawning biomass and yield per recruit calculations over the user-specified years (e.g., last 5 years of the model). This same averaging is also applied to possibly time-varying movement parameters.

For $X\%$ SPR-based reference points, we use a Newton method and iterate

$$\log \widetilde{F}^{(i)} = \log \widetilde{F}^{(i-1)} - \frac{g\left(\log \widetilde{F}^{(i-1)}\right)}{g'\left(\log \widetilde{F}^{(i-1)}\right)} \tag{8}$$

where $g(\log F)$ is the difference between the weighted sums of spawning biomass per recruit at F and $X\%$ of unfished spawning biomass per recruit across stocks:

$$g(\log F) = \sum_{s=1}^{n_s} \lambda_s \left[\phi_s \left(F = e^{\log F}\right) - \frac{X}{100} \phi_s \left(F = 0\right) \right]. \tag{9}$$

where $\phi_s\left(F=0\right)$ is the equilibrium unfished spawning biomass per recruit. $g'(\log F)$ is the derivative of g with respect to $\log F$, and the weights to use for each stock λ_s can be specified by the user or relative to the average of recruitment for each stock over the same years the user defines to calculate "static'' equilibrium spawning biomass and yield.

When a Beverton-Holt or Ricker stock recruit relationship is assumed, an analogous Newton method is used to find $\log F$ that maximizes yield for MSY-based reference points. which are also a functions of the equilibrium yield per recruit (Eq. 7) and equilibrium recruitment. The function $g(\log F)$ in Eq. 8 is the first

derivative of the yield curve with respect to $\log F$.

Projections

The projection options are generally the same as those for previous versions of WHAM (Miller and Stock 2020). When there is movement of any stocks, the user has the option to project and use any random effects for time-varying movement or use the average over user specified years, analogous to how natural mortality can be treated in the projection period. The projection of any environmental covariates has been revised to better include error in the estimated latent covariate in any effects on the population in projection years. Users can also specify a catch or fully-selected fishing mortality in each projection year and they can be fleet-specific.

Application to black sea bass

Black sea bass are a temperate reef fish in the western Atlantic Ocean ranging from the Gulf of Mexico to the Gulf of Maine. Fish north of Cape Hatteras, NC, are considered to comprise a single stock unit, but individual populations exhibit spawning site fidelity (Able and Stanton Hales, Jr. 1997; Fabrizio et al. 2013). Fish in this northern stock unit perform seasonal migrations out on the continental shelf in the fall and back to their inshore spawning areas during the spring (Musick and Mercer 1977). Analyses of tagging studies have demonstrated that the extent of seasonal migration varies along the coast such that fish from populations off of southern New England and further north move offshore and as far south as the coasts of Virgina and North Carolina, whereas fish in the southern portion of the stock range generally move shorter distances between inshore and offshore areas of similar latitude (Moser and Shepherd 2009).

Prior to its 2023 peer-reviewed assessment, the NEUS black sea bass stock was assessed using the Age-Structured Assessment Program (ASAP) model (Legault and Restrepo 1999), a single-stock and -region statistical catch-at-age model that estimates all model parameters as fixed effects. Northern and southern components of the NEUS black sea bass stock ascribed to regions divided by the Hudson Canyon were separately modeled in ASAP (reference map figure). Results from the separate ASAP models were combined for a unit-stock assessment. The ASAP-based assessments exhibited strong retrospective patterns (Mohn 1999), and exploring alternative modeling approaches for the northern and southern stock components has been a high priority for management.

Leading up to the 2023 peer-reviewed assessment, a working group (hereafter referred to as "Working Group")

composed of scientists from federal, state, and academic institutions determined an optimal data and model configuration for the black sea bass stock using the multi-stock and multi-region extension of WHAM described above (NEFSC 2023). This assessment included the spatial features and investigated inclusion of hypothesized environmental drivers that were prioritized research recommendations from previous black sea bass assessments.

Below we describe the assumptions and configuration of the assessment model as determined by the Working Group as well as the alternative assumptions for recruitment and natural mortality in the models we fit to evaluate alternative hypotheses of bottom temperature effects on black sea bass.

Basic structure

The first year being modeled for the population is 1989 and the fishery and index data used in the model span from 1989 to 2021. The north and south stock components are modeled as separate populations that spawn and recruit in respective regions. We have observations for each of four total fishing fleets, where two fishing fleets (recreational and commercial) operate in each region.

There are 11 seasonal intervals within each calendar year: five monthly time intervals from Jan 1 to May 31, a spawning season from June 1 to July 31, and five monthly intervals from August 1 to December 31. The southern stock component is assumed to never move to the northern region. For the northern component, a proportion $\mu_{\mathrm{N}\to\mathrm{S}}$ can move to the southern region each month during the last five months of the year, but no movement is allows from the south to the north during this period (Figure 1). During the first four intervals of the year a proportion $\mu_{\mathrm{S}\to\mathrm{N}}$ the northern component individuals in the south can move back to the north, but no movement from the north to south is allowed during this period. In the fifth interval (May), all northern component individuals remaining in the south are assumed to move back to the north for the subsequent spawning period. Survival and movement occur sequentially in each interval and each of the two movement proportions are assumed constant across intervals, ages, and years.

The two monthly movement matrices are

$$\boldsymbol{\mu}_1 = \begin{bmatrix} 1-\mu_{\mathrm{N}\to\mathrm{S}} & \mu_{\mathrm{N}\to\mathrm{S}} \\ 0 & 1 \end{bmatrix}$$

for the portion of the year after spawning and

$$\boldsymbol{\mu}_2 = \begin{bmatrix} 1 & 0 \\ \mu_{\mathrm{S}\to\mathrm{N}} & 1-\mu_{\mathrm{S}\to\mathrm{N}} \end{bmatrix}$$

for the portion of the year before spawning. As noted in the description of the general WHAM model, tagging data are not yet allowed. However, the Working Group also fit a Stock Synthesis model (Methot and Wetzel 2013) which provided estimated movement rate parameters and standard errors that were used to configure the priors for WHAM (see Supplementary Materials).

With the movement configuration, the northern origin fish (ages 2+) can occur in the southern region on January 1. Estimating initial numbers at age as separate parameters can be challenging even in single-stock models, but for black sea bass the available data cannot distinguish the proportion of northern and southern component fish at each age in the southern region in the initial year of the model. Therefore, we used the simplifying equilibrium assumption described above where there are two parameters estimated for each stock component: an initial recruitment and an equilibrium fully-selected F that determines the abundance at age in each region for each stock component.

For the northern population abundance at age 1 on January 1 (recruitment) is only allowed in the northern region, but given the monthly movement described above, older individuals that previously recruited in the northern region may occur in the southern region on January 1. Therefore, a model with survival random effects will model the transitions (survival/movement) of abundances at age of northern origin fish in each region. All of the initial runs assumed variance parameters for these random effects to be the same for northern origin fish occurring in both regions on January 1. The base model assumes very small variance for the transitions of northern fish in the southern region, which is approximately the same as the deterministic transition assumptions of a statistical catch at age model. We also allow 2DAR1 correlation for recruitment and survival for both the northern and southern components. Unique variance and correlation parameters for the recruitment and survival random effects are estimated for the northern and southern components.

Uncertainty in recreational index observations

The estimated coefficients of variation (CVs) provided by the analyses to generate the recreational catch per angler (recreational CPA) index ranged between 0.02 and 0.06 which the Working Group felt did not capture the true observation uncertainty in the index with regard to its relationship to stock abundance. In many of the initial runs as well as the base model we allowed a scalar multiple of the standard deviation of

the log aggregate index to be estimated for these indices in the northern and southern regions. Models that successfully estimated these scalars indicated standard deviations for these surveys to be approximately 5 times the input value and this value was fixed in many preliminary runs to avoid dealing with convergence problems. However, the base model successfully estimated these scalars. The model estimates are negligibly affected by estimating these scalars, but we felt estimating these parameters allowed uncertainty in model output to be more properly conveyed.

Index and catch age composition observations

The Working Group investigated many alternative assumptions for the probability models and selectivity models for the eight different sets of age composition observations to reduce residual patterns and retrospective patterns. These analyses resulted in use of selectivity random effects for the northern fleet and indices and logistic-normal likelihoods for six sets of of age composition observations and Dirichlet-multinomial likelihoods for one index and one fleet in the northern region (Table S1).

Bottom temperature effects

All model fits also include bottom temperature observations for the northern and southern regions from 1963 to 2021 and estimated standard errors ranging between 0.03 and 0.09 degrees Celsius (NEFSC 2023). We retained the assumption from the peer-reviewed assessment that treated the latent bottom temperature covariates in each region as AR1 processes.

We fit 14 models with alternative assumptions about the effects of bottom temperature covariates, ranging from no effects to effects on both regions for either recruitment or natural mortality at age 1 (Table 1). These analyses derive from the hypothesis that bottom temperature affects overwinter survival of fish where the fish turn from age 0 to age 1 on January 1 (Miller et al. 2016a). This temperature may be a proxy for temperature prior to January 1 and affect survival during the end of the pre-recruit phase or natural mortality in the early part of of the year after becoming age 1. Furthermore, we have no direct observations of age 1 individuals from surveys until the spring season each year. Therefore, we fit models with effects of temperature on recruitment or natural mortality at age 1.

It is standard practice to treat annual recruitment as time-varying deviations from a mean model and all models here treat recruitment deviations as AR1 random effects. However, Miller et al. (2018) showed how inferences of temperature effects on growth or maturity parameters can be very different whether the compared models with and without the effect also include random effects representing residual temporal

variation in parameters. Therefore, we also explored whether including temporal random effects on age 1 natural mortality affected inferences on corresponding temperature effects. Initially, we included random effects on age 1 natural mortality for both the northern and southern stock components, but estimates of these random effects and corresponding variance for the southern component converged to 0 so these were not included in models presented here.

We assume the covariate in year y affects recruitment in the same years because the covariate observations are from months January to March. The fish are technically already 1 year old, but there are no observations of these individuals until later in the year except possibly in fishery catches which are accumulated over the whole year. Expected log-recruitment for a given stock is a linear function of bottom temperature

$$E\left(\log N_{y,1}|x_y\right) = \mu_R + \beta_R x_y. \tag{10}$$

Similarly, expected log-natural morality as a function of bottom temperature is

$$E\left(\log M_{y,1}|x_y\right) = \mu_{M,1} + \beta_M x_y \tag{11}$$

Because age 1 fish for the northern component can exist in both regions after January 1, natural mortality is acting in both regions for this stock. For models with covariate and(or) annual random effects for age 1 fish we assume them only in the northern regions for the northern component. The corresponding random effects are

$$\log N_{y,1} = E\left(\log N_{y,1}|x_y\right) + \varepsilon_{y,1} \tag{12}$$

and

$$\log M_{y,1} = E\left(\log M_{y,1}|x_y\right) + \varepsilon_{M,y}. \tag{13}$$

The constant or mean log-natural mortality rate is assumed to be $\mu_{M,a} = \log(0.4)$ for all ages as recommended by the Working Group. Because the bottom temperature anomalies and random effects are centered at 0, mean log-natural mortality at age 1 over the time series should be approximately equal to $\mu_{M,1}$ for models that include those effects.

Model fitting, diagnostics, reference points, and projections

We used a development version (commit fb8b089) of the WHAM package prior to the release of version 2.0 for all results. All code for fitting models and generating results can be found at

github.com/timjmiller/wham_bsb_paper.

We examined retrospective patterns for all models by fitting corresponding models where the terminal year is reduced sequentially by one year (peel) for seven years. Therefore, there are eight fits of each model with the time series reduced by zero to seven years. We calculated Mohn's ρ for SSB, and average F at ages 6 and 7. Absolute values of Mohn's ρ near 0 imply no pattern in estimation of these quantities as the time-series is sequentially extended.

As in Miller et al. (2016b), we also assessed the consistency of the AIC-based model selection over retrospective peels to guard against previously noted changes in perception of covariate effects on recruitment with increased length of the time series of observations (Myers 1998). This retrospective examination was also recommended by Brooks (2024).

We performed a jitter analysis of the base model M_0 and the best fitting model to investigate whether a local mimimum of the negative log-likelihood surface was obtained by the optimization. We used the jitter_wham function in the WHAM package which by default simulates starting values from a multivariate normal distribution with mean and covariance defined by the MLEs and estimated covariance matrix from the fitted model. See the Supplementary Materials for more details.

For the best performing model, we also performed so-called simulation self-tests where new observations were simulated conditional on all estimated fixed and random effects and the same model configuration was fit to each of the simulated data sets. We estimated median relative bias of SSB across these simulations. See the Supplementary Materials for more details.

We produced SPR-based BRP estimates ($F_{40\%}$ and $\text{SSB}_{40\%}$) from the best performing model using a variety of options provided in WHAM. We generated annual BRP estimates based on the annual weight at age, maturity at age, natural mortality, fleet selectivity, and either the annual recruitment random effect (Eq. 12) or the annual expected recruitment (Eq. 10). We also calculated status as the ratios of annual average F and SSB to the corresponding reference points. Finally, we calculated "prevailing" BRPs using the average weight at age, maturity at age, M, fleet selectivity from the last 5 years (2017 to 2021) and average recruitment over years 2000 to 2021, and made Kobe plots of joint status for the terminal year of the model (2021). All BRPs and status estimates are generated for each region as well as for the total stock.

We projected the best black sea bass model under three alternative scenarios for the bottom temperature covariate where 1) the AR1 time-series model continues into the projection years, 2) the average of the most recent 5 years is projected, and 3) bottom temperature increases in projection years following a prediction from a simple linear regression of the estimated bottom temperature anomalies over time. We specified

fishing mortality in projection years to be constant at the value in the last model year (2021). Average weight, natural mortality, movement, and maturity at age are used in projection years whereas the AR1 processes for all numbers at age random effects are continued.

Results

We found the best model of bottom temperature covariate effects included the effect only on recruitment of the northern stock and no random effects on age 1 natural mortality (M_1, Tables 2 and S2). Model M_1 consistently had the lowest AIC across retrospective peels where the terminal years of data are removed from the model. The difference in AIC for the model that also included bottom temperature effects on recruitment for the southern component (M_3) suggested some evidence for this hypothesis as well. There was little evidence for also including random effects on age 1 natural mortality for the northern stock component. However, when more than three terminal years of data were removed, the evidence for adding age 1 natural mortality random effects for the northern component (M_8) increased is similar to adding bottom temperature effects on southern component recruitment (M_3).

Comparisons of estimates from retrospective peels did not show any indication of differences in model performance. There was very little variation in measures of retrospective patterns for SSB or fishing mortality across models. Mohn's $\rho \approx -0.03$ for SSB of both stock components and Mohn's $\rho \approx 0.03$ and ≈ -0.04 for average F at ages 6 and 7 in north and south regions, respectively (Table 3).

Estimated effects of bottom temperature on recruitment for either the northern or southern component were stable over the retrospective peels and differed negligibly whether effects for each component were estimated in isolation or together (Table 4). The estimates for the effects on each stock component were essentially equivalent whether the effect was on one component or both. Estimates of residual variability in northern component recruitment, as measured by the conditional or marginal standard deviation of the recruitment random effects, increased slightly with the number of peeled years. However, the ratio of standard deviations of models with and without temperature effects was stable with approximately 20% reduction in residual standard deviation when temperature effects were included. The residual variation is reduced because the expected recruitment (Eq. 10) is a function of the covariate (Figure S5).

The posterior estimates of the bottom temperature covariate match the observations well because of the high precision of the observed anomalies (Figure S4). The anomalies for the north and south regions appear highly correlated presumably because of the proximity of the two regions. Because the temperature anomalies are treated as latent variables, other data components in the model can affect the estimated anomalies when

effects on recruitment are included (e.g., Miller et al. 2018), but in this case the estimates of anomalies are altered negligibly during the population model years when the effect on recruitment is estimated (Figure S7).

The effect of the anomalies on expected recruitment can be better observed by comparing the time series of the northern and southern components (Figure 3). The expected recruitment for the southern component without any covariate effects is constant over time whereas the effect on expected recruitment for the northern component induces correlation of the bottom temperature anomalies and expected recruitment. For the northern stock component, most of the lowest estimated recruitment random effects occurred prior to 2000 and several large recruitment estimates occurred after 2010. For the southern stock, recruitment random effect estimates have been less variable and similar to the estimated median particularly since 2005. The estimated stock size of the northern component, as measured by SSB, increased substantially since 2005, whereas that for the southern component peaked in 2002. The increase in the northern component is also reflected in the total size of the combined components. Estimated average total fishing mortality rates across ages 6 and 7 (combining the commercial and recreational fleets) were highest in the southern region prior to 1998 and have declined substantially since then. Estimated fishing mortality rates in the northern region have been less variable, but had largest peaks in 1996, 1999, and 2005. The decline in estimates in the southern component is also reflected in the decline in total fishing mortality across regions.

The estimated movement from the north to the south for the northern stock component is much less than anticipated from the prior distribution that was parameterized based on the companion Stock Synthesis model fit completed by the Working Group (Figure 2). Conversely, the estimated movement rate from south to north was more consistent and slightly greater than that from the companion model. The estimated movement rates varied little across all fitted models implying that the estimation of movement was not sensitive to the alternative assumptions we considered. Furthermore, the very low estimated movement rate from north to south is also consistent with preliminary fits of the WHAM model without the prior distribution where the movement rate was estimated at the lower bound of 0 resulting in a lack of convergence. The estimated movement rates imply that a very small fraction of northern fish are ever in the southern region.

The 2dAR1 random effects for the selectivity parameters of the northern recreational fleet indicate a decrease in selectivity at ages 2 to 6 over the time series which corresponds to increases in the size limits in regulations by states where these catches occurred (Figure 4). The model also estimated a more modest decrease in selectivity at ages 2 to 3 for the northern commercial fleet. The selectivity at the youngest ages for the two fishery independent indices varied over time but without notable trend.

Reference points

Using the expected recruitment rather than the random effects as the multiplier with equilibrium SSB/R results in less variable estimates of annual $SSB_{40\%}$ (Figure 5: top row). Estimates were less variable for the southern stock component than the northern stock component mainly because the expected recruitment is constant for the former whereas that for the northern component varies via the effect of the bottom temperature anomalies. Temporal variation for the southern stock component is mainly caused by annual variation in the inputs to the SSB/R calculation and $F_{40\%}$, but there is also some effect of the variation in the proportion of total recruitment for each stock component as used in the weighting terms to define the 40% reduction in unfished SSB/R (λ_s in Eq. 9). Using the recruitment random effects instead of expected recruitment creates more uncertain estimates of $SSB_{40\%}$ for the southern stock component whereas there is little difference for the northern component because there is less difference in the types of recruitment estimates resulting from the covariate effects (Figure S10).

Ratios of SSB to $SSB_{40\%}$ should be viewed with caution because the SSB reference point is being defined using annual recruitments rather than some form of average recruitment and therefore, ratios larger than 2.5 which would correspond to unfished population sizes are possible (Figure 5: second row). However, for the southern component, using the constant expected recruitment is comparable to using median recruitment and the annual variation in the inputs to SSB/R indicates no years where SSB was greater than unfished levels throughout the time series. The patterns in uncertainty of SSB ratios are the same as those for the SSB reference points (Figure S13).

Differences between annual $F_{40\%}$ estimates using the alternative types of recruitment estimates are much less than those for $SSB_{40\%}$ because the recruitment estimates are only used in the weighting of the stock-specific SSB/R to determine $F_{40\%}$ (λ_s in Eq. 9, Figure 5: third row). For similar reasons, estimates of uncertainty of $F_{40\%}$ are also similar between the type of recruitment estimates (Figure S9). Annual estimates for the northern stock component were lowest in the earliest years of the time series whereas those for the soutern component are relatively stable over time.

For a given type of recruitment used to calculate $F_{40\%}$, the annual ratios of average F to the corresponding reference point are identical for each stock component and in total because of the selectivity used to define a single F reference point across both regions is exactly the same as that for the annual estimate of fishing mortality at age by fleet (Figure 5: fourth row). As for annual $F_{40\%}$, estimates of uncertainty in the ratios are similar whether expected recruitment or the random effects are used to calculate the reference points (Figure S14).

Unlike the annual ratios of F to $F_{40\%}$, the $F_{40\%}$ under prevailing conditions uses a selectivity defined by the average F at age and fleet over the last 5 years, which is different from that of the selectivity in the terminal year and therefore those ratios for each region and in total are different (Figure 5: bottom row). Although the alternative types of recruitment estimates result in different points on the kobe plots for joint status, the uncertainty in the estimates suggest similar probabilities of alternative quadrants. However, the usage of the confidence regions of the ratios to defined probabilities is an approximation because these ratios are functions of both empirical Bayes estimates of random effects as well as maximum likelihood estimates of fixed effects.

Projections

When continuing the AR1 model for the bottom temperature anomalies in the projection years we can see that the uncertainty grows and asymptotes to a level determined by the marginal variance of the process and that the predicted value approaches the estimated marginal mean value of approximately 0 (Figure 6). There is no uncertainty in the projected linear trend because the values were specified as known whereas there is a small level of uncertainty in the projections of the recent average based on the uncertainty in the estimated mean. Comparing projected recruitment for the northern and southern stock components, the projected expected recruitment has much lower uncertainty than the projected random effects regardless of whether bottom temperature affects recruitment. For the northern component, CVs of projected expected recruitment are smaller than those of recruitment random effect, but there are larger differences between CVs of projected expected recruitment assuming AR1 and the other scenarios for the future bottom temperature anomalies are made (Figure S8).

Because projected fishing mortality is specified to be the same as that in the terminal year the same uncertainty is also propagated in the projections (Figure 7). As we would expect, there is no effect of alternative assumptions about bottom temperature in the projections for the southern stock component because the effect of the bottom temperature anomaly is only on the northern component. However, there alternative bottom temperature assumptions do affect projections of northern component SSB and the projections do not stabilize when the anomalies are projected to increase linearly. When the same AR1 assumption for the bottom temperature anomalies is used in projections, CVs of northern and total SSB projections are larger than when the recent average or linear trend are assumed (Figure S8)

Unlike the annual reference points during the model years (prior to 2022), components of the SSB/R calculations are constant in the projection years where the only changing annual values are the recruitments used

in the weighting for $F_{40\%}$ and the recruitments used to calculate the resulting $SSB_{40\%}$ (Figure 8). Estimated reference points in the first few projection years can differ depending on whether the expected recruitment or the random effects are used in their calculation, but longer term projected values are identical because the random effect estimates approach the expected values as the influence of observations diminishes. However, the estimates of uncertainty in the longer term reference points is lower using the expected recruitment rather than the random effects (Figures S9 and S10). The reduction in uncertainty using expected recruitment is less for $F_{40\%}$ than $SSB_{40\%}$ and for the northern component, that includes bottom temperature effects, than the southern component.

Discussion

Black sea bass

In our investigation of bottom temperature effects on recruitment and natural mortality and time-varying random effects on natural mortality at age 1, we found only including effects on recruitment for the northern stock component to be the best model with respect to AIC. Black sea bass in the NEUS is at the northern extent of its range and the estimated increase in expected recruitment with temperature for the northern stock component is consistent with its range extension to the north. Opposite effects of temperature on recruitment or population size would be expected for species in the same general area that are at the southern extent of their range (Gabriel 1992). For example, higher recruitment of the Southern New England-Mid-Atlantic stock of yellowtail flounder is correlated with more cold water persistence into summer fall on the Northeast US shelf Miller et al. (2016b).

Our finding regarding bottom temperature effects is consistent with the bottom temperature effects on recruitment in the assessment model accepted during the peer-review process and which is currently used to assess the stock (NEFSC 2023). However, AIC suggested some weight for models with temperature effects on recruitment for the southern component and random effects on M at age 1. Although this might suggest making inferences on the population by using an ensemble of these and weighting by AIC (Burnham and Anderson 2002), the estimates of assessment outputs relevant for management (e.g., SSB and F) were similar among the models and weighted estimates would differ very little from the estimates with the lowest AIC.

We showed that using expected recruitment rather than recruitment random effects to define BRPs can produce the same estimates but with lower uncertainty. Using expected bottom temperature anomalies rather than the random effects would also result in the same BRPs, but presumably with even less uncertainty

than those we showed using expected recruitment. These results can be important for management when uncertainty in assessment output is used in making catch advice. The typical approach for defining stock and harvest status is to compare BRPs defined under prevailing conditions with current stock and harvest levels, but we could also make the comparisons with projected BRPs like those we demonstrated are possible. The uncertainty in these ratios could also be used in defining catch advice.

For black sea bass, it is evident that the projection methodology of the environmental covariate has an impact on short-term projection estimates of recruitment and SSB (Figure 6). In the projection period, the AR1 approach reverts to the long-term mean of the environmental covariate. This is most likely not an appropriate assumption for stocks in the NEUS given observations and hypothesis of increasing water temperature and changing environmental conditions (Hare 2016; Pershing et al. 2021). Because of these concerns, the most recent stock assessment for yellowtail flounder used a change point analysis on environmental covariates to determine current conditions. The mean environmental covariate from the current condition was then used as a data input in WHAM to inform short-term projections (NEFSC, 2024). Unfortunately, this methodology still has limitations because it is unlikely that current environmental conditions are stable. Similarly, a linear increase of temperature is also not likely in the future (see past trends, Figure 6 top row).As more assessments begin including effects of environmental covariates explicitly in assessment models, assumptions about these covariates in calculated BRPs and population projections becomes an important decision in the management process.

General Model aspects

WHAM provides a large class of models for time- and age-varying random effects for population attributes and treatment of environmental covariates and their effects on populations using state-space methods (Maunder 2024). This framework accounts for the magnitude of differing uncertainties in observations and stochastic population dynamics processes. Version 2.0 extends these inferences to movement rates for multi-region models and stock (component) specific configuration of random and environmental covariate effects.

Future developments

An obvious limitation to WHAM is the inability to include tagging observations of any type. Such observations are critical to estimation of movement parameters (e.g., Goethel et al. 2019). We used estimates of movement parameters from a companion assessment model to define prior distributions for corresponding movement parameters in the state-space black sea bass model, but other than the tagging data, both of the

assessment models used much the same data which can lead to inappropriate inferences. A better approach would be to estimate the movement parameters externally from just the tagging data.

Tagging data can also inform mortality rate parameters (Hampton 1991). It is well known that natural mortality is seldom estimated in assessment models because the observed data often provide little information to distinguish natural mortality from other assessment model parameters (Lee et al. 2011; Clark 2022). Estimation of natural mortality may be even more challenging within state-space assessment models with their greater flexibility from inclusion of time-varying random effects. For example, we fixed the mean natural mortality for age 1 fish and Cadigan (2016) and Stock et al. (2021) also estimated natural mortality deviations. Therefore allowing tagging observations in WHAM should be a high priority even for models with a single stock and region. This extension would also be beneficial for black sea bass because the current assessment uses much the same data to estimate movement outside of the model as we are using to estimate the other parameters in the WHAM model.

WHAM version 2.0 only currently allows models where each stock spawns and recruits in a single region however, many stocks are assessed with spatial units that are assumed to have a global stock and recruitment model that distributes recruitment to each region (references). Therefore, extending WHAM to allow such models would be beneficial. Similarly age composition data are scarce for many stocks incorporating the work by Correa et al. (2023) on allowing length composition and modeling growth within WHAM would provide an assessment tool to include process errors in assessment with such data and possibly with multiple stocks and regions.

Conclusions

WHAM version 2.0 extends the existing R package to allow multiple stocks and discrete spatial regions. It allows autocorrelated random effects and environmental covariate effects on movement rates. Estimates of movement rates from auxiliary studies can be used to construct prior distributions for movement rates in lieu of integrated likelihoods for tagging data. Version 2.0 also allows seasonal treatment of different fishing fleets and movement of individual stocks, and internal estimation of SPR- and MSY-based reference points accounting for seasonal spatial dynamics including movement and mortality and any environmental covariate effects.

We applied this extended version to investigate alternative hypotheses about effects of bottom temperature on recruitment and age 1 natural mortality for black sea bass. Our analyses indicate evidence for effects of bottom temperature on recruitment for the northern component represents was stronger than other models

that included effects on age 1 mortality and/or corresponding effects on the southern stock component.

Future WHAM development should prioritize including tagging data to inform stock assessment parameter estimation and merging in the version created by Correa et al. (2023) to allow modeling of growth and inclusion of length and length-at-age composition observations.

References

Able, K.W., and Stanton Hales, Jr., L. 1997. Movements of juvenile black sea bass *Centropristis striata* (linnaeus) in a southern New Jersey estuary. Journal of Experimental Marine Biology and Ecology **213**(2): 153–167. doi:10.1016/S0022-0981(96)02743-8.

Andersen, P.K., and Keiding, N. 2002. Multi-state models for event history analysis. Statistical Methods in Medical Research **11**: 91–115. doi:10.1191/0962280202SM276ra.

Arnason, A.N. 1972. Parameter estimates from mark-recapture experiments on two populations subject to migration and death. Researches on Population Ecology **13**: 97–113. doi:10.1007/BF02521971.

ASMFC. 2016. Black sea bass stock assessment. Available at http://www.asmfc.org/uploads/file/5953f11d2016BlackSeaBassS

Bell, R.J., Richardson, D.E., Hare, J.A., Lynch, P.D., and Fratantoni, P.S. 2015. Disentangling the effects of climate, abundance, and size on the distribution of marine fish: An example based on four stocks from the Northeast US shelf. ICES Journal of Marine Science **72**(5): 1311–1322. doi:10.1093/icesjms/fsu217.

Bosley, K.M., Schueller, A.M., Goethel, D.R., Hanselman, D.H., Fenske, K.H., Berger, A.M., Deroba, J.J., and Langseth, B.J. 2022. Finding the perfect mismatch: Evaluating misspecification of population structure within spatially explicit integrated population models. Fish and Fisheries **23**(2): 294–315. doi:10.1111/faf.12616.

Brooks, E.N. 2024. Pragmatic approaches to modeling recruitment in fisheries stock assessment: A perspective. Fisheries Research **270**: 106896. doi:10.1016/j.fishres.2023.106896.

Burnham, K.P., and Anderson, D.R. 2002. Model selection and multimodel inference: A practical information-theoretic approach. Springer-Verlag, New York.

Cadigan, N.G. 2016. A state-space stock assessment model for northern cod, including under-reported catches and variable natural mortality rates. Canadian Journal of Fisheries and Aquatic Sciences **73**(2): 296–308. doi:10.1139/cjfas-2015-0047.

Cao, J., Truesdell, S.B., and Chen, Y. 2014. Impacts of seasonal stock mixing on the assessment of Atlantic cod in the Gulf of Maine. ICES Journal of Marine Science **71**(6): 1443–1457. doi:10.1093/icesjms/fsu066.

Clark, W.G. 2022. Why natural mortality is estimable, in theory if not in practice, in a data-rich stock

assessment. Fisheries Research **248**: 106203. doi:10.1016/j.fishres.2021.106203.

Commenges, D. 1999. Multi-state models in epidemiology. Lifetime Data Analysis **5**: 315–327. doi:10.1023/A:1009636125294.

Correa, G.M., Monnahan, C.C., Sullivan, J.Y., Thorson, J.T., and Punt, A.E. 2023. Modelling time-varying growth in state-space stock assessments. ICES Journal of Marine Science **80**(7): 2036–2049. doi:10.1093/icesjms/fsad133.

Fabrizio, M.C., Manderson, J.P., and Pessutti, J.P. 2013. Habitat associations and dispersal of black sea bass from a Mid-Atlantic Bight reef. Marine Ecology Progress Series **482**: 241–253. doi:10.3354/meps10302.

Francis, R.I.C.C. 2014. Replacing the multinomial in stock assessment models: A first step. Fisheries Research **151**: 70–84. doi:10.1016/j.fishres.2013.12.015.

Gabriel, W.L. 1992. Persistence of demersal fish assemblages between Cape Hatteras and Nova Scotia, Northwest Atlantic. Journal of the Northwest Atlantic Fisheries Science **14**(1): 29–46.

Goethel, D.R., Bosley, K.M., Hanselman, D.H., Berger, A.M., Deroba, J.J., Langseth, B.J., and Schueller, A.M. 2019. Exploring the utility of different tag-recovery experimental designs for use in spatially explicit, tag-integrated stock assessment models. Fisheries Research **219**: 105320. doi:10.1016/j.fishres.2019.105320.

Hampton, J. 1991. Estimation of southern bluefin tuna *Thunnus maccoyii* natural mortality and movement rates from tagging experiments. Fishery Bulletin **89**(4): 591–610.

Hare, W.E.A.N., Jonathan A. AND Morrison. 2016. A vulnerability assessment of fish and invertebrates to climate change on the northeast u.s. Continental shelf. PLOS ONE **11**: 1–30. doi:10.1371/journal.pone.0146756.

Hearn, W.S., Sundland, R.L., and Hampton, J. 1987. Robust estimation of the natural mortality rate in a completed tagging experiment with variable fishing intensity. Journal Du Conseil International Pour L'exploration De La Mer **43**: 107–117. doi:10.1093/icesjms/43.2.107.

Kapur, M.S., Siple, M.C., Olmos, M., Privitera-Johnson, K.M., Adams, G., Best, J., Castillo-Jordán, C., Cronin-Fine, L., Havron, A.M., Lee, Q., Methot, R.D., and Punt, A.E. 2021. Equilibrium reference point calculations for the next generation of spatial assessments. Fisheries Research **244**: 106132. doi:10.1016/j.fishres.2021.106132.

Kemeny, J.G., and Snell, J.L. 1960. Finite markov chains. D. Van Nostrand Company, Princeton, New Jersey.

Kristensen, K., Nielsen, A., Berg, C., Skaug, H., and Bell, B.M. 2016. TMB: Automatic differentiation and Laplace approximation. Journal of Statistical Software **70**: 1–21. doi:10.18637/jss.v070.i05.

Lee, H.-H., Maunder, M.N., Piner, K.R., and Methot, R.D. 2011. Estimating natural mortality within a fish-

eries stock assessment model: An evaluation using simulation analysis based on twelve stock assessments. Fisheries Research **109**(1): 89–94. doi:10.1016/j.fishres.2011.01.021.

Legault, C.M., and Restrepo, V.R. 1999. A flexible forward age-structured assessment program. Col. Vol. Sci. Pap. ICCAT **49**(2): 246–253.

Maunder, M.N. 2024. Towards a comprehensive framework for providing management advice from statistical inference using population dynamics models. Ecological Modelling **498**: 110836. doi:10.1016/j.ecolmodel.2024.110836.

Methot, R.D., and Wetzel, C.R. 2013. Stock Synthesis: A biological and statistical framework for fish stock assessment and fishery management. Fisheries Research **142**(1): 86–99. doi:10.1016/j.fishres.2012.10.012.

Miller, A.S., Shepherd, G.R., and Fratantoni, P.S. 2016a. Offshore habitat preference of overwintering juvenile and adult black sea bass, *Centropristis striata*, and the relationship to year-class success. PLOS ONE **11**(1): e0147627. doi:10.1371/journal.pone.0147627.

Miller, T.J., and Andersen, P.K. 2008. A finite-state continuous-time approach for inferring regional migration and mortality rates from archival tagging and conventional tag-recovery experiments. Biometrics **64**(4): 1196–1206. doi:10.1111/j.1541-0420.2008.00996.x.

Miller, T.J., Hare, J.A., and Alade, L.A. 2016b. A state-space approach to incorporating environmental effects on recruitment in an age-structured assessment model with an application to southern New England yellowtail flounder. Can. J. Fish. Aquat. Sci. **73**(8): 1261–1270. doi:10.1139/cjfas-2015-0339.

Miller, T.J., O'Brien, L., and Fratantoni, P.S. 2018. Temporal and environmental variation in growth and maturity and effects on management reference points of Georges Bank Atlantic cod. Can. J. Fish. Aquat. Sci. **75**(12): 2159–2171. doi:10.1139/cjfas-2017-0124.

Miller, T.J., and Stock, B.C. 2020. The Woods Hole Assessment Model (WHAM). https://timjmiller.github.io/wham.

Mohn, R. 1999. The retrospective problem in sequential population analysis: An investigation using cod fishery and simulated data. ICES Journal of Marine Science **56**(4): 473–488. doi:10.1006/jmsc.1999.0481.

Moser, J., and Shepherd, G.R. 2009. Seasonal distribution and movement of black sea bass (*Centropristis striata*) in the Northwest Atlantic as determined from a mark-recapture experiment. Journal of Northwest Atlantic Fishery Science **40**: 17–28.

Musick, J.A., and Mercer, L.P. 1977. Seasonal distribution of black sea bass, *Centropristis striata*, in the Mid-Atlantic Bight with comments on the ecology and fisheries of the species. Transactions of the American Fisheries Society **106**(1): 12–25. doi:10.1577/1548-8659(1977)106<12:SDOBSB>2.0.CO;2.

Myers, R.A. 1998. When do environment–recruitment correlations work? Reviews in Fish Biology and Fisheries **8**(3): 229–249. doi:10.1023/A:1008828730759.

NEFSC. 2022a. Final report of the haddock research track assessment working group. Available at

https://s3.us-east-1.amazonaws.com/nefmc.org/14b_EGB_Research_Track_Haddock_WG_Report_DRAFT.pdf.

NEFSC. 2022b. Report of the american plaice research track working group. Available at https://s3.us-east-1.amazonaws.com/nefmc.org/2_American-Plaice-WG-Report.pdf.

NEFSC. 2023. Report of the black sea bass (*Centropristis striata*) research track stock assessment working group. Available at https://www.mafmc.org/s/a_2023_BSB_UNIT_RTWG_Report_V2_12_2_2023-1.pdf.

NEFSC. 2024. Butterfish research track assessment report. US Dept Commer Northeast Fish Sci Cent Ref Doc. 24-03; 191 p.

Nielsen, A., and Berg, C.W. 2014. Estimation of time-varying selectivity in stock assessments using state-space models. Fisheries Research **158**: 96–101. doi:10.1016/j.fishres.2014.01.014.

Perreault, A.M.J., Wheeland, L.J., Morgan, M.J., and Cadigan, N.G. 2020. A state-space stock assessment model for American plaice on the Grand Bank of Newfoundland. Journal of Northwest Atlantic Fishery Science **51**: 45–104. doi:10.2960/j.v51.m727.

Pershing, A.J., Alexander, M.A., Brady, D.C., Brickman, D., Curchitser, E.N., Diamond, A.W., McClenachan, L., Mills, K.E., Nichols, O.C., Pendleton, D.E., Record, N.R., Scott, J.D., Staudinger, M.D., and Wang, Y. 2021. Climate impacts on the Gulf of Maine ecosystem: A review of observed and expected changes in 2050 from rising temperatures. Elementa: Science of the Anthropocene **9**(1): 00076. doi:10.1525/elementa.2020.00076.

Punt, A.E., Dunn, A., Elvarsson, B., Hampton, J., Hoyle, S.D., Maunder, M.N., Methot, R.D., and Nielsen, A. 2020. Essential features of the next-generation integrated fisheries stock assessment package: A perspective. Fisheries Research **229**: 105617. doi:10.1016/j.fishres.2020.105617.

Schwarz, C.J., Schweigert, J.F., and Arnason, A.N. 1993. Estimating migration rates using tag-recovery data. Biometrics **49**: 177–193. doi:10.2307/2532612.

Stock, B.C., and Miller, T.J. 2021. The Woods Hole Assessment Model (WHAM): A general state-space assessment framework that incorporates time- and age-varying processes via random effects and links to environmental covariates. Fisheries Research **240**: 105967. doi:10.1016/j.fishres.2021.105967.

Stock, B.C., Xu, H., Miller, T.J., Thorson, J.T., and Nye, J.A. 2021. Implementing two-dimensional autocorrelation in either survival or natural mortality improves a state-space assessment model for Southern New England-Mid Atlantic yellowtail flounder. Fisheries Research **237**: 105873. doi:10.1016/j.fishres.2021.105873.

Sullivan, M.C., Cowen, R.K., and Steves, B.P. 2005. Evidence for atmosphere–ocean forcing of yellowtail flounder (*Limanda ferruginea*) recruitment in the Middle Atlantic Bight. Fisheries Oceanography **14**(5): 386–399. doi:10.1111/j.1365-2419.2005.00343.x.

Thorson, J.T., Johnson, K.F., Methot, R.D., and Taylor, I.G. 2017. Model-based estimates of effective sample size in stock assessment models using the Dirichlet-multinomial distribution. Fisheries Research **192**: 84–93. doi:10.1016/j.fishres.2016.06.005.

Thorson, J.T., Miller, T.J., and Stock, B.C. 2023. The multivariate-tweedie: A self-weighting likelihood for age and length composition data arising from hierarchical sampling designs. ICES Journal of Marine Science **80**(10): 2630–2641. doi:10.1093/icesjms/fsac159.

Varkey, D.A., Babyn, J., Regular, P., Ings, D.W., Kumar, R., Rogers, B., Champagnat, J., and Morgan, M.J. 2022. A state-space model for stock assessment of cod (gadus morhua) stock in NAFO subdivision 3Ps. DFO Can. Sci. Advis. Sec. Res. Doc. 2022/022. v + 78 p.

Ying, Y., Chen, Y., Lin, L., and Gao, T. 2011. Risks of ignoring fish population spatial structure in fisheries management. Canadian Journal of Fisheries and Aquatic Sciences **68**(12): 2101–2120. doi:10.1139/f2011-116.

Figures

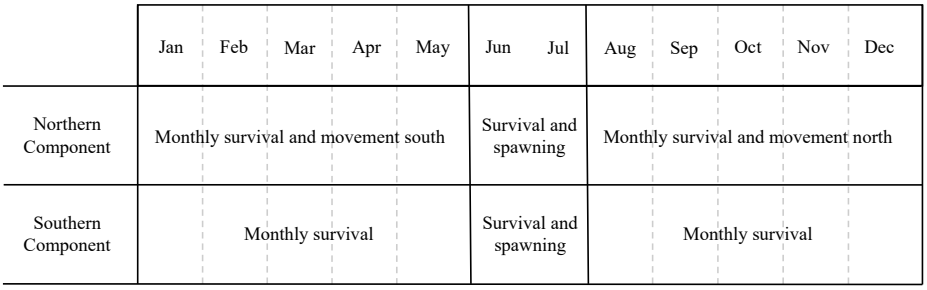

Figure 1: Diagram of intervals within the year and configuation of the dynamics of each component of the BSB population.

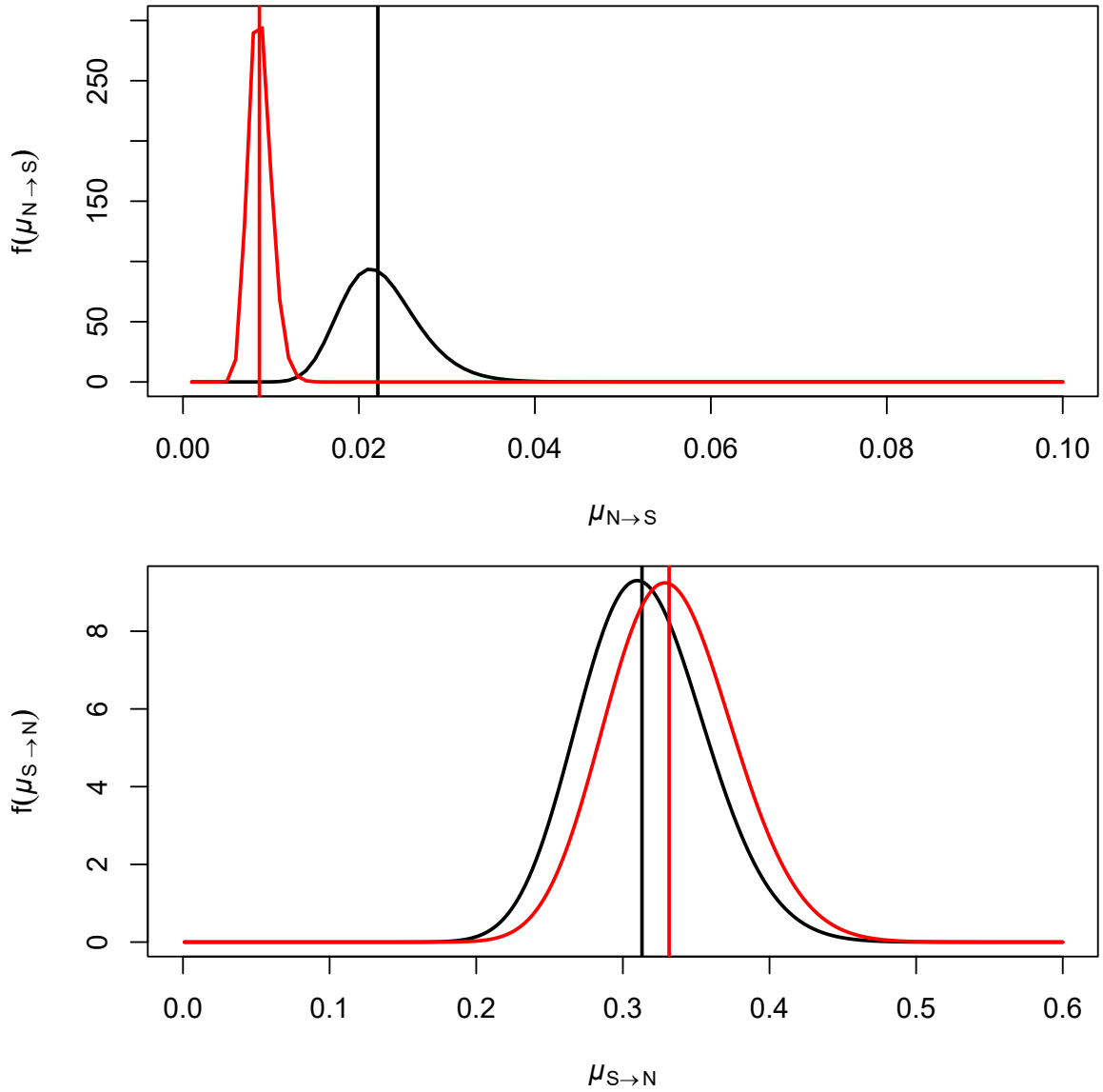

Figure 2: Prior (black) and posterior (red) distributions of movement of northern component stock from north to south (top) and south to north (bottom).

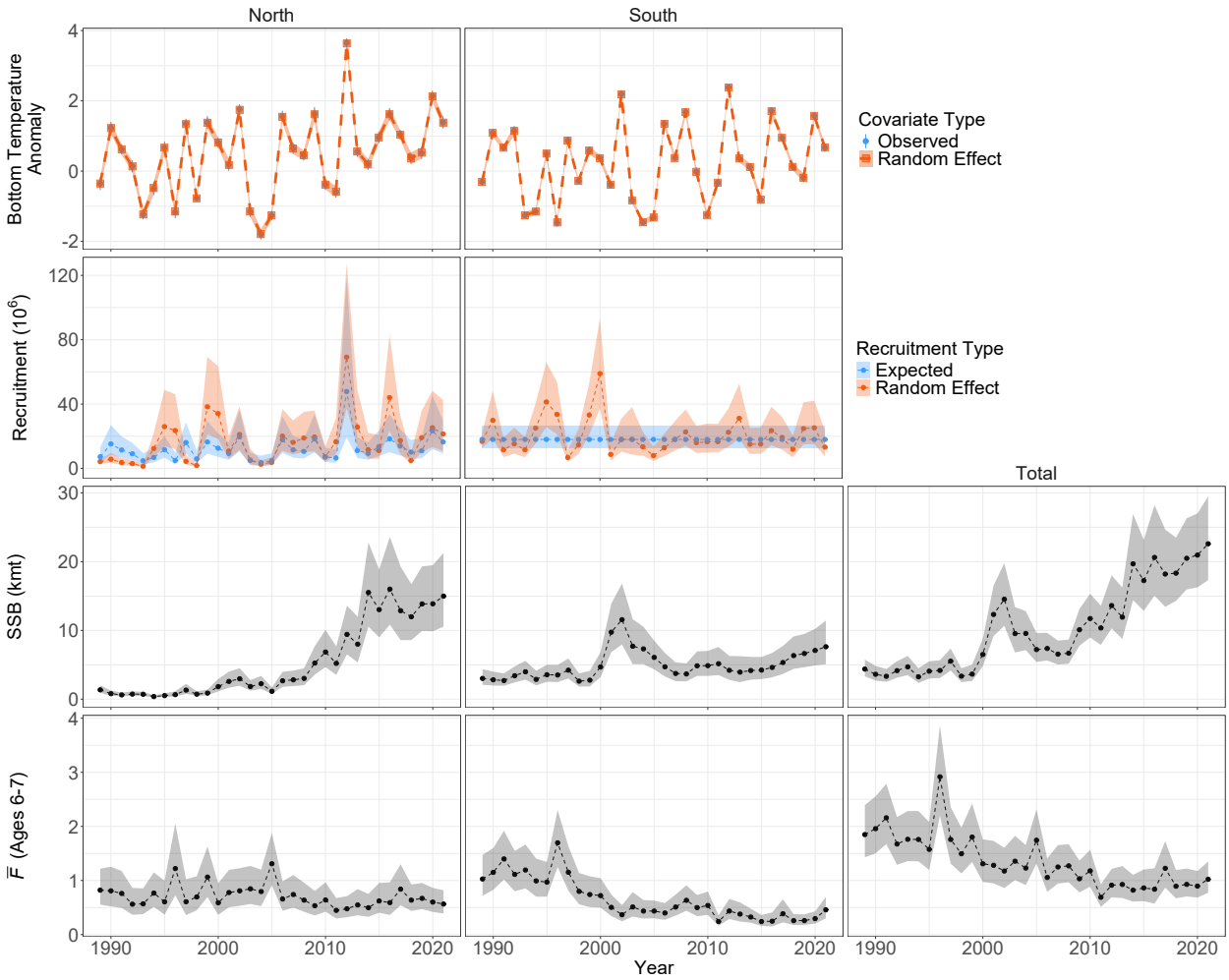

Figure 3: Annual observations and posterior estimates of bottom temperature anomalies (top row), annual expected and random effect recruitment estimates (second row) and SSB and average fishing mortality at ages 6 and 7 from model M_1. Columns define estimates regionally (spawning region for SSB) and toal SSB and fishing mortality across regions. Polygons and vertical lines represent 95% confidence intervals.

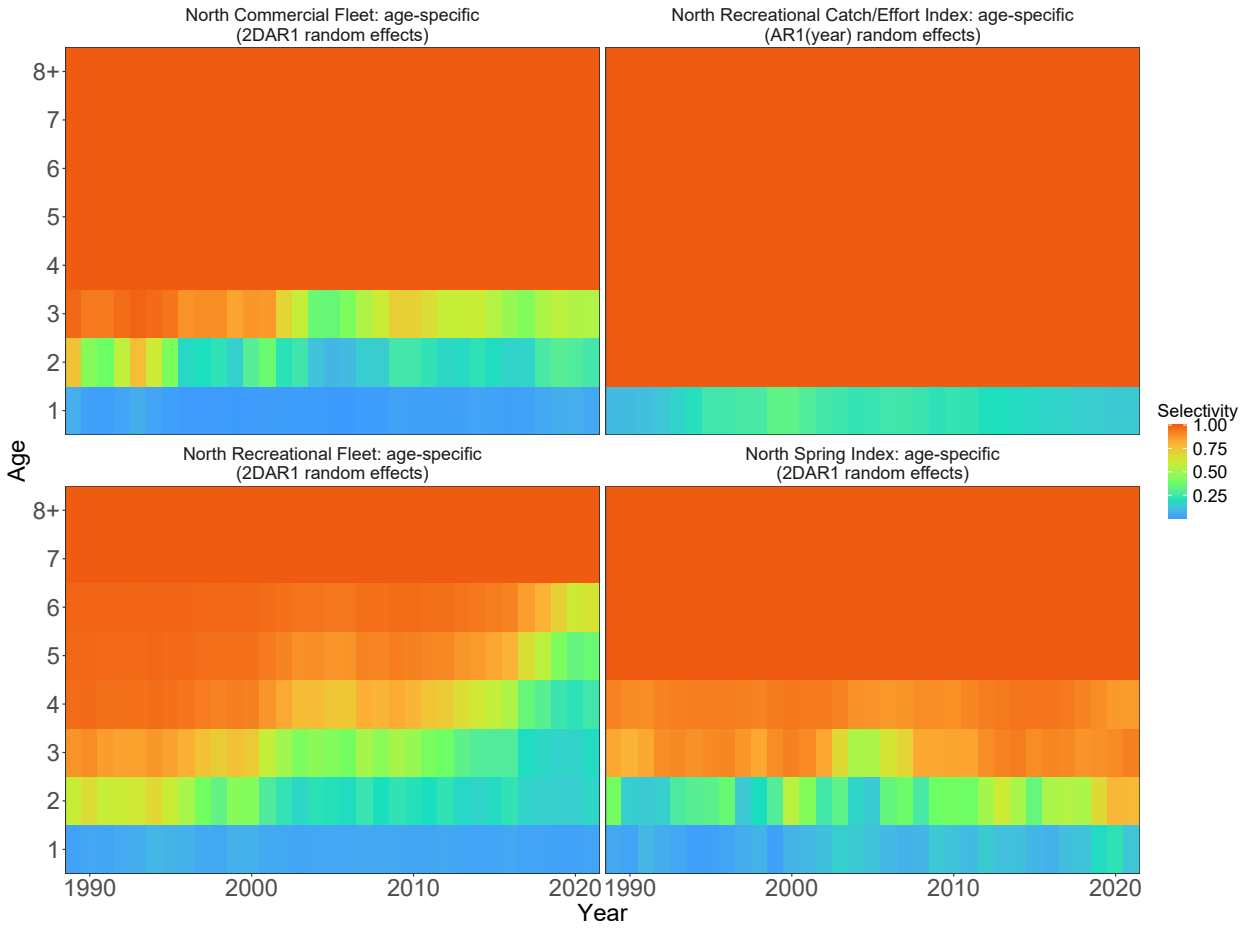

Figure 4: Time and age-varying selectivty for fleets and indices in the northern region with autoregressive random effects.

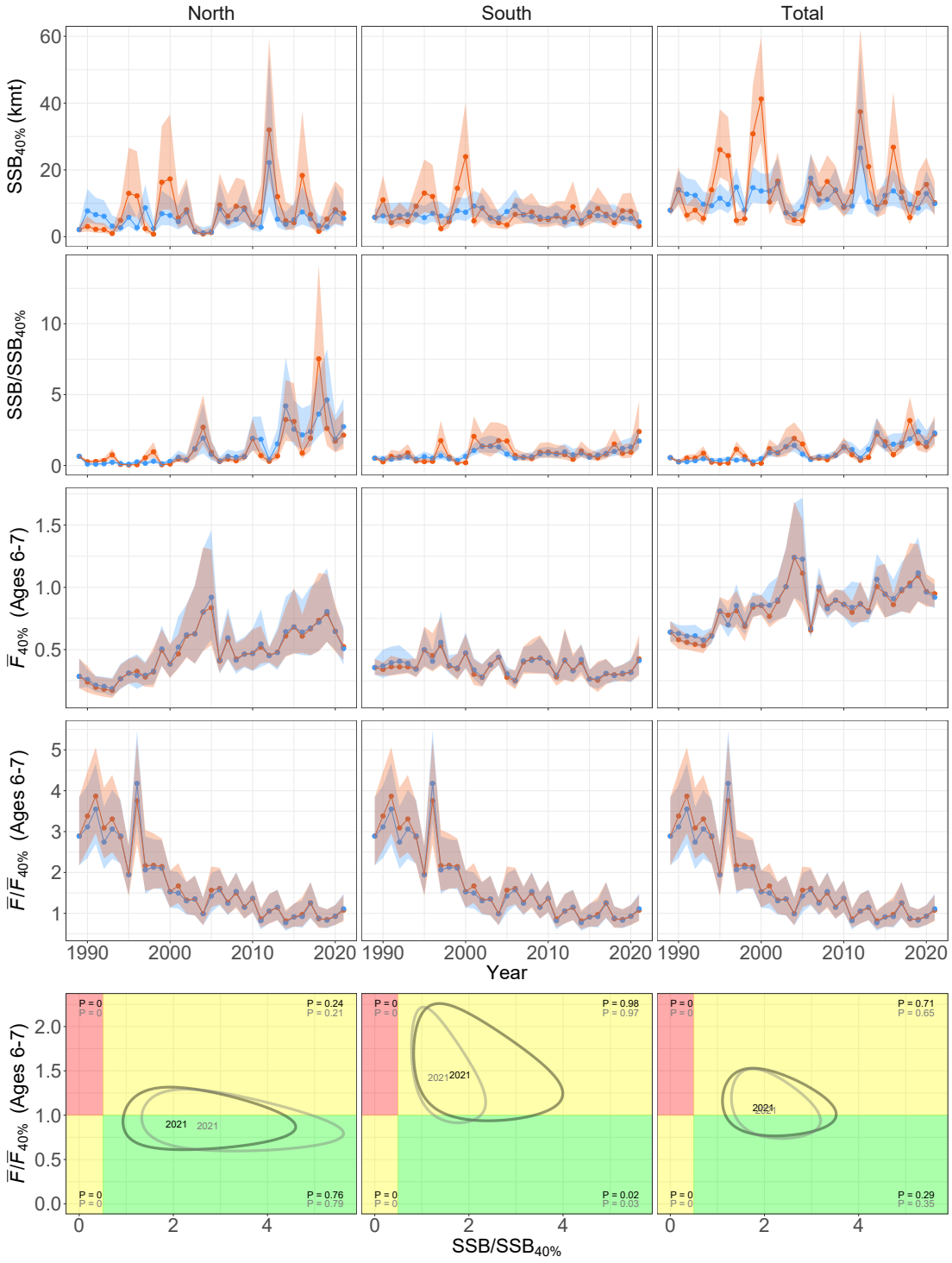

Figure 5: Estimates of average equilibrium F at ages 6 and 7 that produces the 40% spawning potential ratio, equilibrium SSB at $F_{40\%}$ based on annual inputs to SSB/R calculations, annual fishing and biomass status (ratios), and bivariate kobe plots of status in 2021 where reference points represent prevailing conditions with inputs to SSB/R averaged over the last 5 years and recruitment is averaged over the time series. Red and blue in first 4 rows and black and gray in final row indicate alternative annual estimates of recruitment (random effect or expected). All results are based on model M_1. Polygons represent 95% confidence intervals or regions.

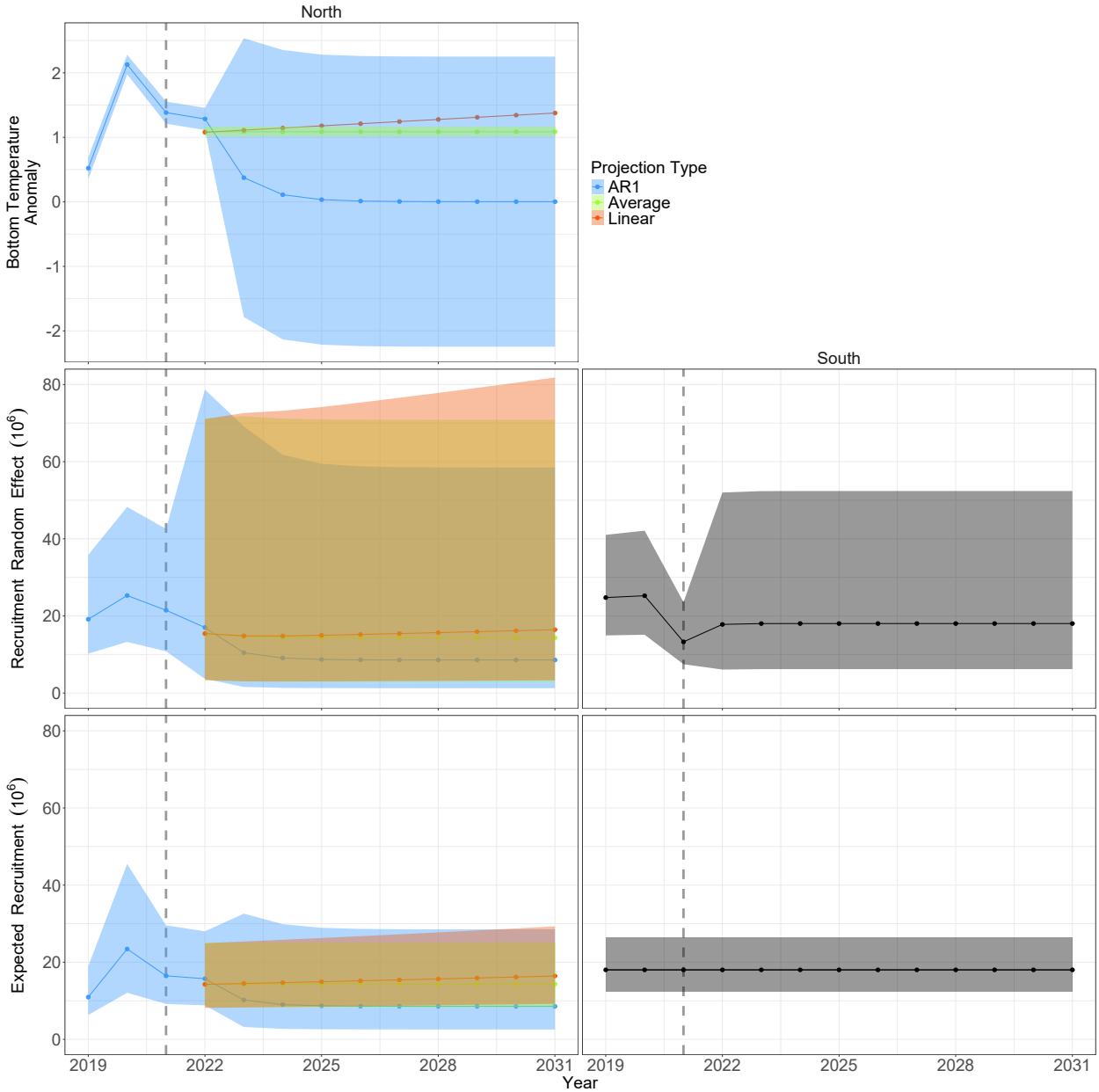

Figure 6: Annual estimates of bottom temperature in the northern region and alternative recruitment estimates (random effect or expected) by region. Estimates from years after 2021 are from projections of model $M1$ under three alternative assumptions for the bottom temperature anomalies in the northern region. Vertical dotted line is the last year of data and polygons represent 95% confidence intervals.

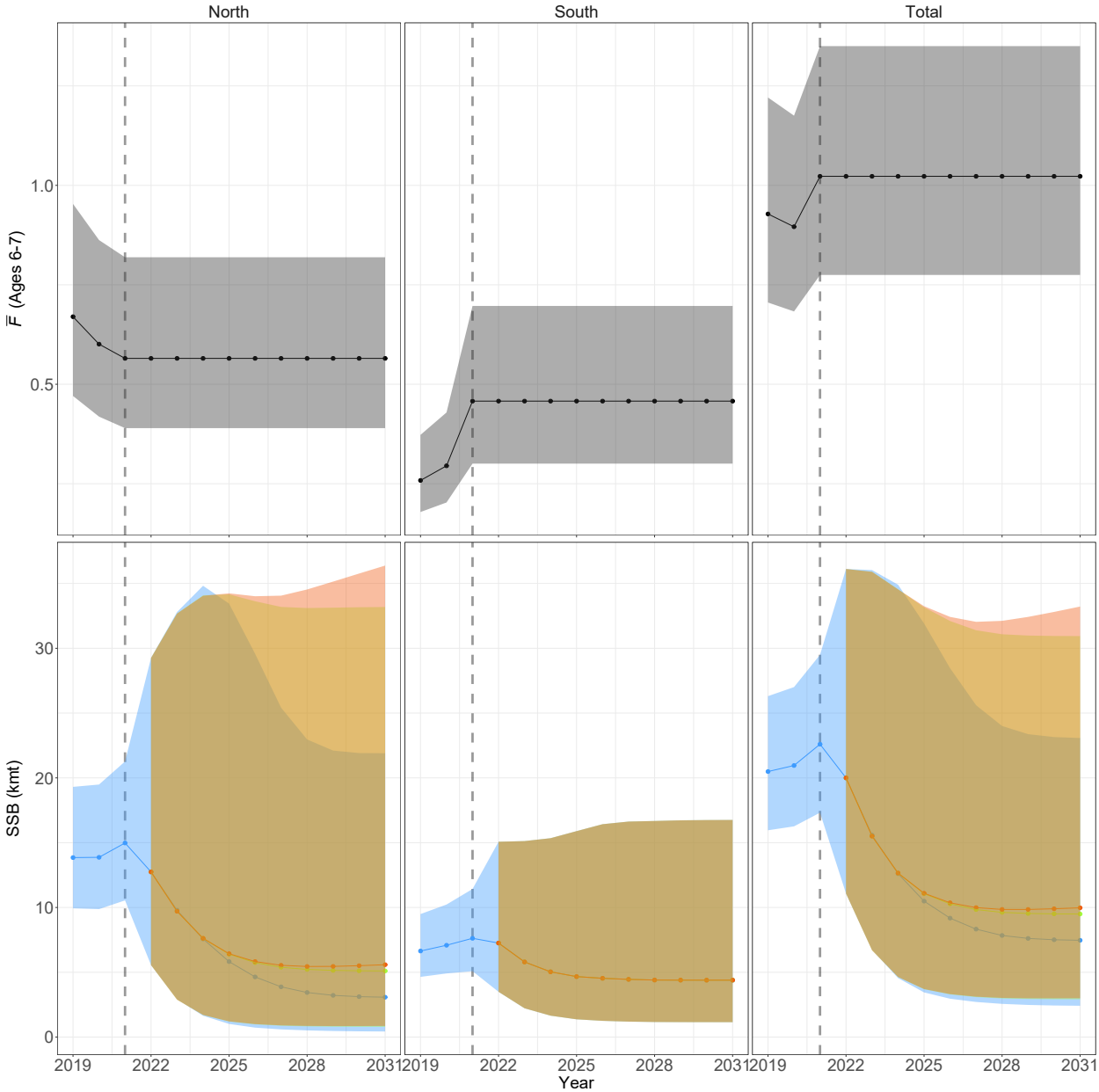

Figure 7: Annual estimates of average fishing mortality and SSB by region and in total. Estimates in years beyond 2021 are from projecting model M_1 under alternative assumptions for bottom temperature anomalies in the northern region. Vertical dotted line is the last year of data and polygons represent 95% confidence intervals.

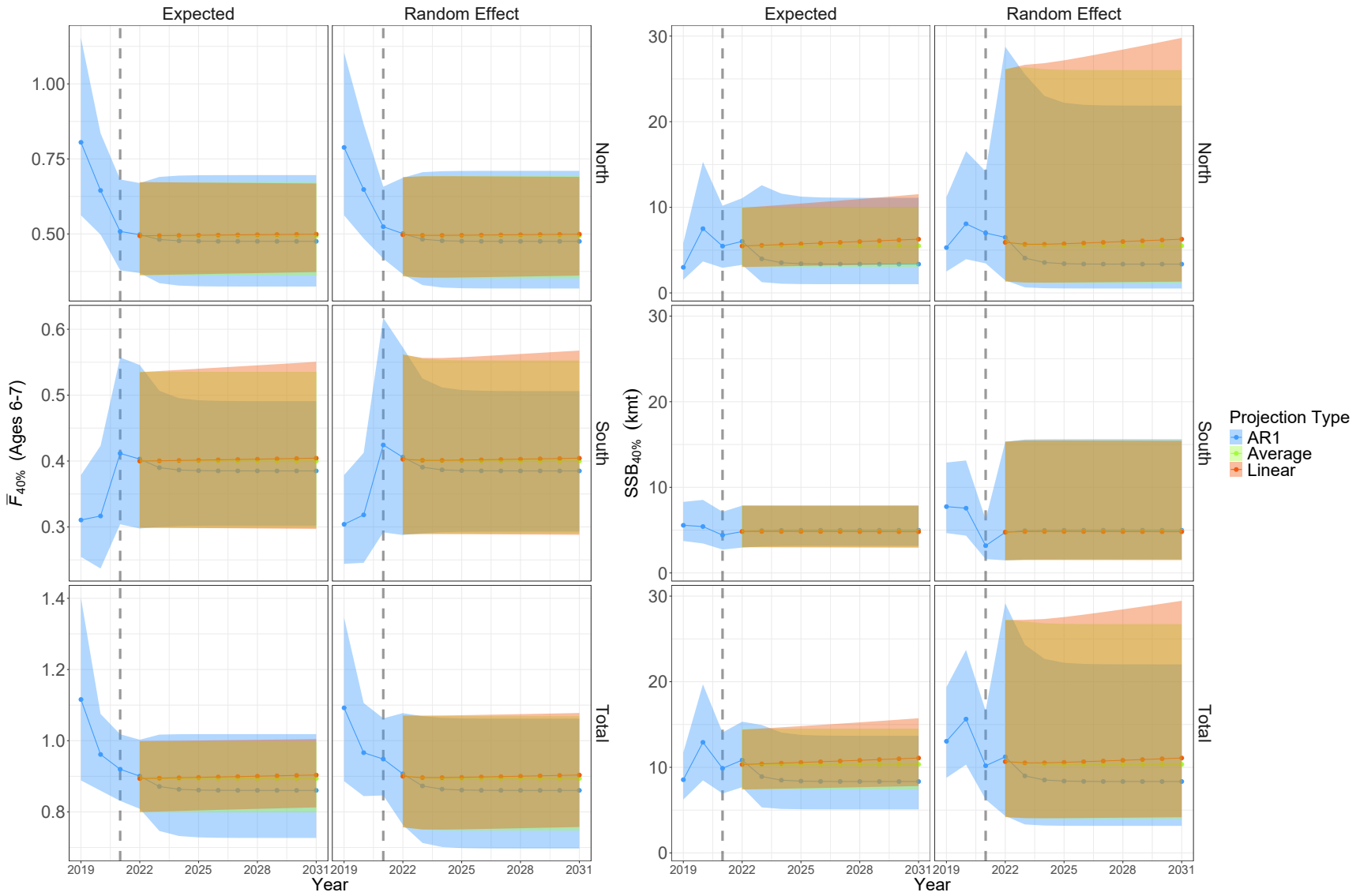

Figure 8: Annual estimates by region and in total of average equilibrium F at ages 6 and 7 that produces the 40% spawning potential ratio and SSB at $F_{40\%}$. Estimates in years beyond 2021 are from projecting model M_1 under alternative assumptions for bottom temperature anomalies in the northern region and average SSB/R inputs from the last 5 years of the unprojected model. Vertical dotted line is the last year of data and polygons represent 95% confidence intervals.

Tables

Table 1: Assumptions for temperature effects and random effects for age 1 natural mortality for each model.

	Temperature Effect		
Model	North	South	M at age 1 random effects
M_0	–	–	none
M_1	Recruitment	–	none
M_2	–	Recruitment	none
M_3	Recruitment	Recruitment	none
M_4	M at age 1	–	none
M_5	–	M at age 1	none
M_6	M at age 1	M at age 1	none
M_7	–	–	time-varying
M_8	Recruitment	–	time-varying
M_9	–	Recruitment	time-varying
M_{10}	Recruitment	Recruitment	time-varying
M_{11}	M at age 1	–	time-varying
M_{12}	–	M at age 1	time-varying
M_{13}	M at age 1	M at age 1	time-varying

Table 2: Difference between AIC and the lowest AIC for each model by retrospective peel.

	Peel							
Model	0	1	2	3	4	5	6	7
M_0	11.83	11.39	10.41	10.05	9.86	9.41	8.47	8.22
M_1	0.00	0.00	0.00	0.00	0.00	0.00	0.00	0.00
M_2	12.63	12.03	11.41	11.06	10.91	10.34	9.20	9.22
M_3	0.80	0.64	1.00	1.01	1.05	0.93	0.73	1.00
M_4	13.81	13.35	12.26	11.82	11.71	11.18	10.08	9.85
M_5	13.25	12.55	11.68	11.21	11.07	10.41	9.86	9.71
M_6	15.22	14.51	13.52	12.97	12.91	12.17	11.46	11.33
M_7	14.32	13.75	12.17	11.30	11.43	10.55	9.71	9.42
M_8	2.25	2.10	1.47	0.96	1.29	0.91	0.98	0.99
M_9	15.12	14.39	13.17	12.31	12.48	11.49	10.44	10.43
M_{10}	3.05	2.74	2.47	1.97	2.34	1.84	1.71	1.99
M_{11}	16.29	15.74	14.17	13.30	13.43	12.55	11.68	11.39
M_{12}	15.73	14.91	13.43	12.46	12.64	11.55	11.10	10.92
M_{13}	17.70	16.91	15.43	14.46	14.64	13.55	13.07	12.88

Table 3: Mohn's ρ for SSB, and average F at ages 6 and 7 in northern and southern regions.

	SSB		Average F	
Model	North	South	North	South
M_0	-0.040	-0.023	0.041	-0.048
M_1	-0.040	-0.023	0.041	-0.048
M_2	-0.040	-0.024	0.041	-0.047
M_3	-0.040	-0.024	0.041	-0.047
M_4	-0.041	-0.022	0.042	-0.048
M_5	-0.041	-0.023	0.042	-0.048
M_6	-0.042	-0.023	0.042	-0.048
M_7	-0.042	-0.022	0.043	-0.048
M_8	-0.044	-0.023	0.044	-0.048
M_9	-0.042	-0.024	0.043	-0.048
M_{10}	-0.044	-0.024	0.044	-0.047
M_{11}	-0.041	-0.022	0.042	-0.048
M_{12}	-0.042	-0.023	0.043	-0.048
M_{13}	-0.041	-0.023	0.042	-0.048

Table 4: Estimates of temperature effects on recruitment and variance and autocorrelation parameters for recruitment for northern (N) and southern (S) components for models with no effects (M_0), effects on specific components (M_1 and M_2) or both components simultaneously (M_3) from the full model (Peel 0) and each retrospective peel.

	Peel							
Parameter	0	1	2	3	4	5	6	7
M_1 $\widehat{\beta}_{R,N}$	0.474	0.480	0.485	0.476	0.464	0.468	0.439	0.445
M_2 $\widehat{\beta}_{R,S}$	0.099	0.105	0.094	0.095	0.092	0.096	0.099	0.091
M_3 $\widehat{\beta}_{R,N}$	0.474	0.480	0.485	0.476	0.464	0.468	0.439	0.445
M_3 $\widehat{\beta}_{R,S}$	0.099	0.105	0.094	0.095	0.092	0.096	0.099	0.091
M_0 Conditional $\widehat{\sigma}_{R,N}$	0.925	0.953	0.978	0.988	0.978	1.010	0.981	1.007
M_1 Conditional $\widehat{\sigma}_{R,N}$	0.730	0.752	0.780	0.786	0.775	0.801	0.785	0.800
M_0 $\widehat{\rho}_{R,N}$	0.362	0.375	0.385	0.405	0.424	0.432	0.427	0.431
M_1 $\widehat{\rho}_{R,N}$	0.296	0.307	0.334	0.373	0.394	0.406	0.428	0.429
M_0 Marginal $\widehat{\sigma}_{R,N}$	0.992	1.028	1.060	1.080	1.081	1.120	1.084	1.117
M_1 Marginal $\widehat{\sigma}_{R,N}$	0.764	0.791	0.827	0.848	0.843	0.877	0.869	0.885

Appendix A

Table A1: Definition of terms.

i	Seasonal time interval
δ_i	Length of seasonal time interval i
a	Age class
y	Year
A	Last age class ("plus group")
r	Region
f	Fishing fleet
n_F	Number of fishing fleets
s	Stock
n_R	Number of regions
$\mathbf{P}_{y,a,i}$	Probability transition matrix for year y, age a, and season i
$\mathbf{O}_{y,a,i}$	submatrix of $\mathbf{P}_{y,a,i}$ of probabilities of surviving and occuring in each region for year y, age a, and season i
$\mathbf{H}_{y,a,i}$	submatrix of $\mathbf{P}_{y,a,i}$ of probabilities of being captured in each fishing fleet for year y, age a, and season i
$\mathbf{I}_H$	n_f x n_f identity matrix
m	Index observation
$O_{y,a,i}(r,r')$	For year y, age a and season i, the probability of surviving and occurring in region r' given beginning the interval alive in region r
$H_{y,a,i}(r,f)$	For year y, age a and season i, the probability of being captured in fleet f given beginning the interval alive in region r
$S_{y,a,i}$	For year y, age a and season i, the probability of surviving the interval (1 region model)
$F_{y,a,i,f}$	Fishing mortality rate for fleet f in year y at age a in seasonal interval i
$M_{y,a}$	Natural mortality rate in year y at age a (single region)
$M_{y,a,r}$	Natural mortality rate in region r and year y at age a
$Z_{y,a,i}$	Total mortality rate in year y at age a in seasonal interval i (single region)
$Z_{y,a,i,r}$	Total mortality rate in region r and year y at age a in seasonal interval i
$\mathbf{S}_{y,a,i}$	matrix of of probabilities of surviving in each region over the interval for season i, year y, age a

Table A1: (Continued)

$\boldsymbol{\mu}_{y,a,i}$	matrix of of probabilities of moving or staying in each region at the end of season i in year y and age a
$\mu_{r\to r',y,a,i}$	For year y, age a and seasonal interval i, either the probability of moving at the end of the interval or instantanteous rate of movement from region r to region r'
r_f	region where fleet f operates
$\mathbf{N}_{y,a}$	Column vector of abundances by region at age a in year y
$\mathbf{A}_{y,a,i}$	instantaneous rate matrix for seasonal interval i, year y, and age a
$a_{y,a,i,r}$	For year y, age a and seasonal interval i, the hazard or negative sum of the instantaneous rates of mortality and movement from the state corresonding to being alive in region r
$\mathbf{P}_{y,a}(\delta_1,\ldots,\delta_K)$	Probability transition matrix for year y and age a over seasonal intervals $\delta_1,\ldots,\delta_K$
K	Number of seasons in the annual time step
t_s	fraction of the annual time step when spawning occurs for stock s
$\delta_{s,j}$	fraction of the annual time step between t_s and the end of season $j-1$
t_m	fraction of the annual time step when index m observers the population
$\delta_{m,j}$	fraction of the annual time step between t_m and the end of season $j-1$
$\mathbf{N}_{y,a}$	Abundance at age a in year y in each of the living and mortality states on January 1
$\mathbf{N}_{O,y,a}$	Abundance at age a in year y alive in each region on January 1
$N_{y,a,r}$	Abundance at age a in year y alive in region r on January 1
r_s	region where stock s spawns and recruits
$\mathrm{SSB}_{s,y}$	Spawning stock biomass for stock s in year y
$\varepsilon_{y,a,r}$	Random error for abundance at age a in year y in region r
$w_{s,y,a}$	mean individual weight for stock s at age a in year y
$\mathrm{mat}_{s,y,a}$	proportion mature at age a in year y for stock s
$\mathbf{O}_{s,y,a,r_s}(t_s)$	Probabilities of surviving and occurring in region r_s at time t_s given being alive in each region at the start of the year
$\boldsymbol{\varepsilon}_{y,a}$	vector of random errors for abundance alive in each region on January 1 of year y at age a
$\sigma_{N,r}$	standard deviation parameter for abundance at age random effects in region r
$\rho_{N,\mathrm{age},r}$	first order auto-regressive correlation parameter across age for abundance at age random effects in region r
$\rho_{N,\mathrm{year},r}$	first order auto-regressive correlation parameter across year for abundance at age random effects in region r

Table A1: (Continued)

$\text{sel}_{1,a,f}$	selectivity at age a for fleet f in the first year
$F_{1,a,f}$	fishing mortality rate at age a for fleet f in the first year
$\widetilde{F}_{a,f}$	equilibrium fishing mortality rate at age a for fleet f
$\mathbf{O}_a$	proportion surviving the year at age j and occuring in each region (columns) given alive on January 1 in each region (rows)
$\widetilde{\mathbf{O}}_a$	equilibrium proportions alive in each region at age a (columns) given recruitment in each region (rows)
$\mathbf{N}_{O,1,r}$	vector of abundance by age in region r in the first year
$\theta_{N_1,r}$	mean parameter for initial numbers at age random effects in the first year for region r
$\boldsymbol{\varepsilon}_{N_1,r}$	vector of random effects by age for initial numbers at age in the first year for region r
$\sigma_{N_1,r}$	standard deviation parameter for initial numbers at age random effects in the first year for region r
$\rho_{N_1,r}$	first order auto-regressive correlation parameter for initial numbers at age random effects in the first year for region r
$\mu_{r\to r',y,a,i}$	movement from region r to region r' in seasonal interval i and year y at age a
$g(\mu_{r\to r',y,a,i})$	link function for movement $\mu_{r\to r',y,a,i}$
$\theta_{r\to r',i}$	mean parameter across age and year for movement from region r to region r' in seasonal interval i
$\varepsilon_{r\to r',y,a,i}$	random effect parameter for movement from region r to region r' in seasonal interval i and year y at age a
n_E	number of environmental covariates
$\beta_{r\to r',a,i,k}$	effect of environmental covariate k on movement from region r to r' at age a in seasonal interval i
$E_{k,y}$	latent environmetal covariate k affecting the population in year y
$\sigma_{r\to r',i}$	standard deviation parameter for movement random effects from region r to r' in seasonal interval i
$\rho_{r\to r',\text{age},i}$	first order auto-regressive correlation parameter across age for movement random effects from region r to r' in seasonal interval i
$\rho_{r\to r',\text{year},i}$	first order auto-regressive correlation parameter across year for movement random effects from region r to r' in seasonal interval i

Table A1: (Continued)

$\gamma_{r\to r',i}$	random effect for link-transformed mean movement from region r to r' in seasonal interval i when a prior distribution is assumed
$\sigma_{r\to r',i}$	standard deviation parameter for prior distribution of $\gamma_{r\to r',i}$
$M_{y,a,r}$	natural mortality rate for age a in year y in region r
$\theta_{M,r}$	mean parameter across age and year for nutural mortality in region r
$\varepsilon_{M,r,y,a}$	random effect parameter for natural mortality in region r and year y at age a
$\beta_{M,r,a,k}$	effect of environmental covariate k on natural mortality in region r at age a
$\sigma_{M,r}$	standard deviation parameter for natural mortality random effects in region r
$\rho_{M,\text{age},r}$	first order auto-regressive correlation parameter across age for natural mortality random effects in region r
$\rho_{M,\text{year},r}$	first order auto-regressive correlation parameter across year for natural mortality random effects in region r
$\widehat{\mathbf{N}}_{H,s,y,a}$	vector of predicted numbers of stock s at age a in year y captured by each fleet
$\widehat{\mathbf{N}}_{H,y,a}$	vector of predicted numbers at age a in year y captured by each fleet across all stocks
$\widehat{\mathbf{C}}_{y,a}$	vector of predicted biomass captured at age a in year y by each fleet across all stocks
$\mathbf{c}_{y,a}$	vector of mean individual weight at age a in year y for each fleet
$\widehat{\mathbf{C}}_{y}$	vector of predicted aggregate catch for each fleet in year y
$C_{y,f}$	observed aggregate catch for fleet f in year y
$\widehat{C}_{y,f}$	predicted aggregate catch for fleet f in year y
$\sigma_{y,f}$	standard deviation of observed log-aggregate catch for fleet f in year y
$\widehat{N}_{s,y,a,m}$	predicted abundance at t_m in region r_m
$\mathbf{O}_{s,y,a,r_m}(t_m)$	the probabilities of surviving and occurring in region r_m at time t_m given being alive in each region at the start of the year which is the r_m column of the upper-left submatrix of Eq. 4
$\widehat{I}_{m,y,a}$	Predicted relative abundance index for survey d in year y at age a
$q_{m,y}$	catchability of index m in year y
$\text{sel}_{m,y,a}$	selectivity of index m at age a in year y
$w_{m,y,a}$	average weight of individuals at age a for index m if the index is quantified in biomass, otherwise it is unity
u_m	upper bound for index m catchability
l_m	lower bound for index m catchability
$\theta_{q,m}$	mean index m catchability parameter

Table A1: (Continued)

$\varepsilon_{q,m,y}$	index m catchability random effect in year y
$\beta_{q,m,k}$	effect of environmental covariate k on index m catchability
$\sigma_{q,r}$	standard deviation parameter for index m catchability random effects
$\rho_{q,m}$	first order auto-regressive correlation parameter across year for index m catchability random effects

Supplemental Materials

Deriving the prior distribution for movement parameters

The Working Group fit a Stock Synthesis model (Methot and Wetzel 2013) that included tagging data with 2 seasons (6 months each) and 2 regions where a proportion μ_1^* of the northern component moves to the south in one season and some proportion $\mu_{2\to1}^*$ move back to the south in the second season (NEFSC 2023). The seasonal movement matrices for each season are

$$\boldsymbol{\mu}_1^* = \begin{bmatrix} 1-\mu_{1\to2}^* & \mu_{1\to2}^* \\ 0 & 1 \end{bmatrix}$$

and

$$\boldsymbol{\mu}_2 = \begin{bmatrix} 1 & 0 \\ \mu_{2\to1}^* & 1-\mu_{2\to1}^* \end{bmatrix}.$$

To obtain estimates of movement proportions for the monthly intervals in the WHAM model, the half-year movement matrices were converted to monthly movement matrices by taking the root z_k of $\boldsymbol{\mu}_k^*$ which are defined by the number of months of movement for each season (5 and 4, respectively). The roots of the matrices are calculated using an eigen decomposition of the matrices

$$\boldsymbol{\mu}_k = (\boldsymbol{\mu}_k^*)^{z_k} = \mathbf{V}_k \mathbf{D}_k^{z_k} \mathbf{V}_k^{-1}$$

where $z_1 = 1/5$ for and $z_2 = 1/4$, and $\mathbf{V}_k$ and $\mathbf{D}_k$ are the matrix of eigenvectors (columnwise) and the diagonal matrix of corresponding eigenvalues of $\boldsymbol{\mu}_k^*$. The Working Group used a parametric bootstrap approach to determine an appropriate standard deviation for the prior distribution for the movement parameters. Stock Synthesis also estimates parameters on a transformed scale, but different from WHAM:

$$\mu_{r\to r'}^* = \frac{1}{1+2e^{-x_{r\to r'}}}$$

The estimated parameters and standard errors from the Stock Synthesis model were $x_{1\to2} = -1.44$ and $x_{2\to1} = 1.94$ and $SE(x_{1\to2})) = 0.21$ and $SE(x_{2\to1})) = 0.37$. The resulting in the estimated proportions were $\mu_{1\to2}^* = 0.11$ and $\mu_{2\to1}^* = 0.78$.

In WHAM, an additive logit transformation is used which is simply a logit transformation when there are

only two regions:

$$\mu_{r\to r'} = \frac{1}{1+e^{-y_{r\to r'}}}.$$

We simulated 1000 values from a normal distribution with mean and standard deviation defined by the parameter estimate and standard error $\tilde{x}_{r\to r',b} \sim N(x_{r\to r'}, SE(x_{r\to r'}))$ from the Stock Synthesis model. For each simulated value we constructed $\tilde{\boldsymbol{\mu}}^*_{r\to r',b}$, took the appropriate root and calculated inverse logit for $\tilde{y}_{r\to r',b}$. We calculated the mean and standard deviation of the values $y_{i,b}$. The mean values did not differ meaningfully from the transformation of the original estimates ($y_{1\to 2} = -3.79$ and $y_{2\to 1} = -0.79$) and the standard deviation was approximately 0.2 for both parameters.

Diagnostics

Jitter fits for model M_0

WHAM by default completes three newton steps after the stats::nlminb minimization function completes to reduce the gradient at the minimized NLL. However, this generally has negligible effects on model estimates and the NLL. To reduce computation time, we did not complete these newton steps when performing jitter fits of the model. Without the Newton steps, the maximum (absolute) gradient sizes are generally less than 0.01 for models that converge satisfactorily.

The 50 jitter fits demonstrated that a local minimum was obtained for the original fit of model M_0 (Figure S1). Some lower NLLs were obtained with unacceptable gradients, but a slightly lower NLL was found with a satisfactory gradient and with and invertible hessian. We therefore refit model M_0 and all remaining models using the better parameter estimates as initial values.

Jitter fits for model M_1

The 50 jitter fits gave no evidence of a better minimization of the NLL. Three lower NLLs were obtained, but with unacceptably large gradients (Figure S2). The largest differences in parameter estimates for these three jitters were for numbers at age and selectivity random effects variance and correlation parameters.

Self test for model M_1

Initial fits to simulated data from model M_1 showed estimation of the observation error standard deviation multiplier for the recreational catch-per angler indices in the north and south regions was unstable. Many

of the fits to the simulated data produced implausible estimates at the 0 boundary for these parameters (very negative values on log-scale). Therefore, we completed self-tests with these parameters fixed at the true values.

For 7 of the the simulated data sets the model failed to optimize. The maximum absolute gradient was $< 10^{-6}$ for only 9 and $< 10^{-4}$ for 52 of the 93 successfully fitted models. The poor convergence appeared to be attributable to the estimation of the scalar for the standard errors of the log-transformed northern Recreational CPA index for which estimates tended to 0 for nearly all of the fits (< 0.01 for 83 fits). However, even across all fits including those with poor convergence, the SSB estimates appeared to be reliable (Figure S3).

Table S1: Configuration of age composition likelihoods, mean selectivity models, and selectivity random effects models for each age composition data component. For all logistic-normal likelihoods, any ages observed as zeros are treated as missing.

Data component	Age Composition Likelihood	Mean Selectivity model	Random effects Model
North commercial fleet	Dirichlet-Multinomial	age-specific (ages > 3 fully selected)	AR1 correlation by age and year
North recreational fleet	Logistic-normal (Independent)	age-specific (ages > 6 fully selected)	AR1 correlation by age and year
South commercial fleet	Logistic-normal (AR1 correlation)	logistic	None
South recreational fleet	Logistic-normal (AR1 correlation)	logistic	None
North recreational CPA index	Logistic-normal (Independent)	age-specific (ages > 1 fully selected)	AR1 correlation by year
North VAST index	Dirichlet-Multinomial	age-specific (ages > 4 fully selected)	AR1 correlation by age and year
South recreational CPA index	Logistic-normal (AR1 correlation)	age-specific (ages > 2 fully selected)	None
South VAST index	Logistic-normal (AR1 correlation)	age-specific (ages > 1 fully selected)	None

Table S2: Model AIC weights for each retrospective peel.

	Peel							
Model	0	1	2	3	4	5	6	7
M_0	0.00	0.00	0.00	0.00	0.00	0.00	0.01	0.01
M_1	0.45	0.43	0.42	0.38	0.41	0.37	0.36	0.38
M_2	0.00	0.00	0.00	0.00	0.00	0.00	0.00	0.00
M_3	0.30	0.31	0.25	0.23	0.24	0.23	0.25	0.23
M_4	0.00	0.00	0.00	0.00	0.00	0.00	0.00	0.00
M_5	0.00	0.00	0.00	0.00	0.00	0.00	0.00	0.00
M_6	0.00	0.00	0.00	0.00	0.00	0.00	0.00	0.00
M_7	0.00	0.00	0.00	0.00	0.00	0.00	0.00	0.00
M_8	0.15	0.15	0.20	0.24	0.21	0.24	0.22	0.23
M_9	0.00	0.00	0.00	0.00	0.00	0.00	0.00	0.00
M_{10}	0.10	0.11	0.12	0.14	0.13	0.15	0.15	0.14
M_{11}	0.00	0.00	0.00	0.00	0.00	0.00	0.00	0.00
M_{12}	0.00	0.00	0.00	0.00	0.00	0.00	0.00	0.00
M_{13}	0.00	0.00	0.00	0.00	0.00	0.00	0.00	0.00

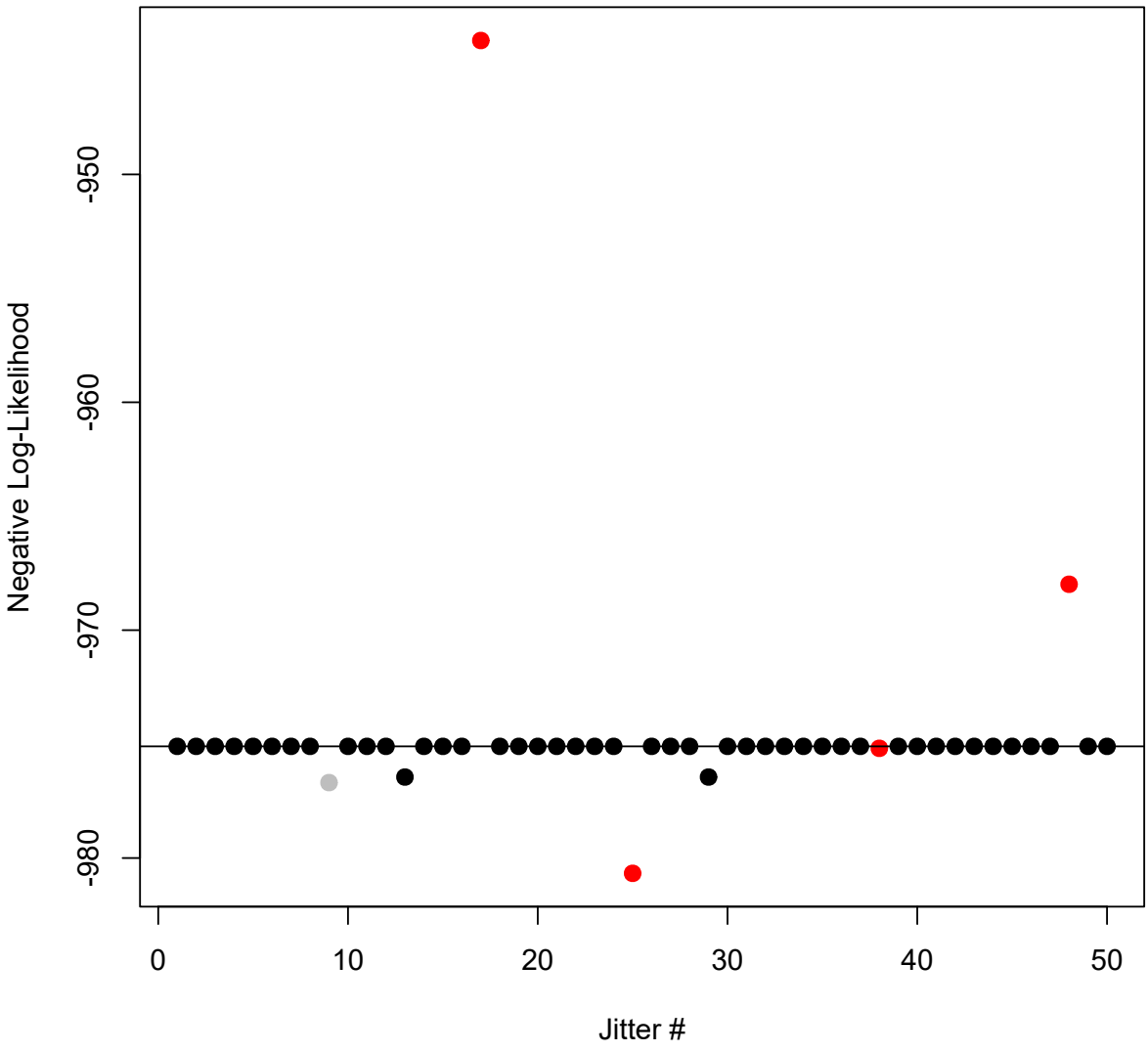

Figure S1: Minimized negative log-likelihood for 50 fits where minimization used initial parameter values jittered from those provided by an initial fit for model M_0. Black jitters had maximum absolute gradient values $< 10^{-10}$, grey jitters had values $> 10^{-10}$ and < 1, and red jitters had values > 1.

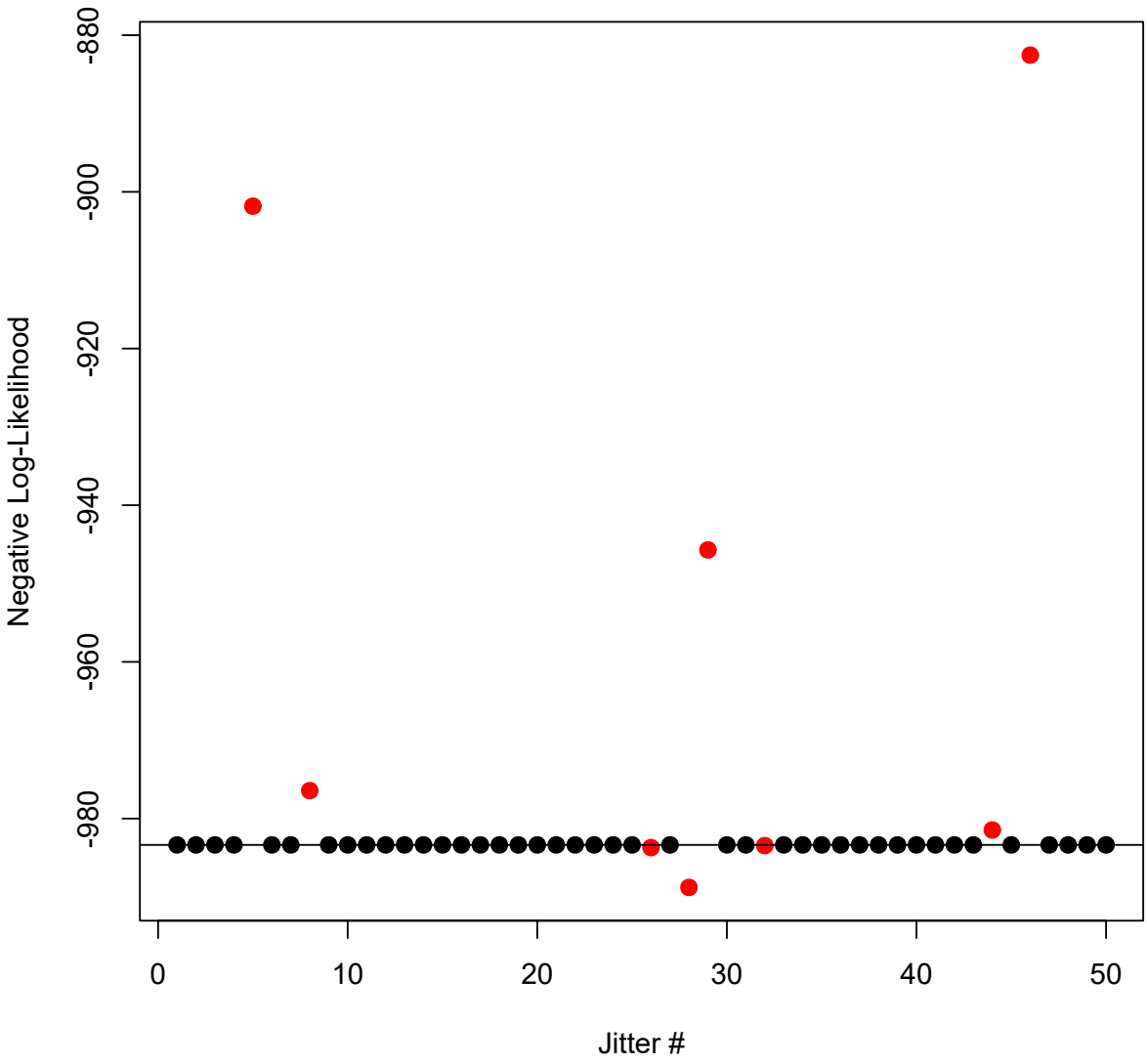

Figure S2: Minimized negative log-likelihood for 50 fits where minimization used initial parameter values jittered from those provided by an initial fit for model M_1. Fits with black dots had maximum absolute gradient value < 0.01 and fits with red dots had values > 10.

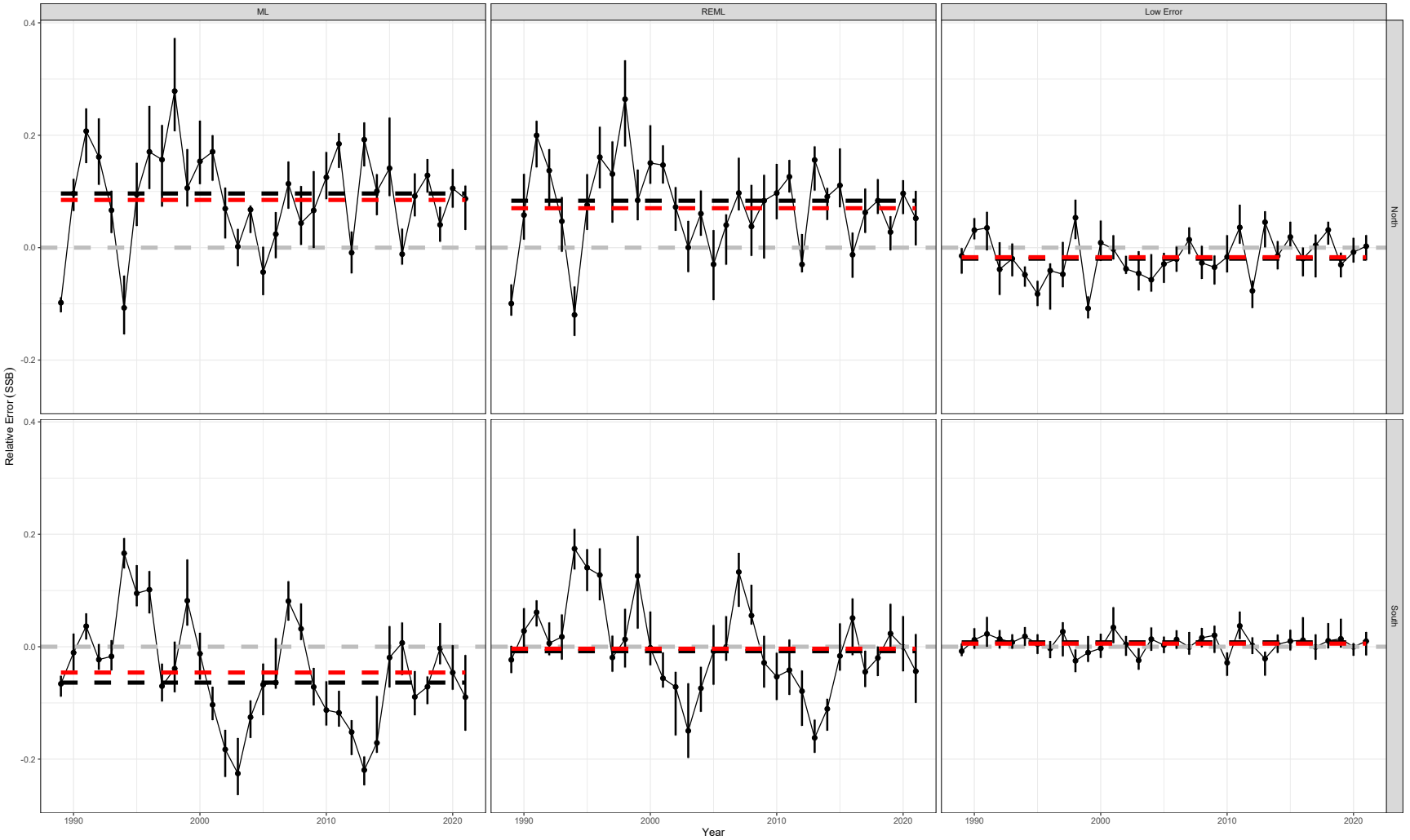

Figure S3: Median relative bias of SSB for the North and South stock components for estimation models where the observation variance of log-indices are fixed and estimation is by maximum marginal likelihood (ML) or Restricted Maximum Likelihood (REML) or where the standard deviation of logistic-normal age composition observations are assumed to be 0.1 (over sqrt(1000)) (Low Error). Black and Red dashed lines represent the median of the yeaerly medians and the median across all yearly relative errors, respectively.

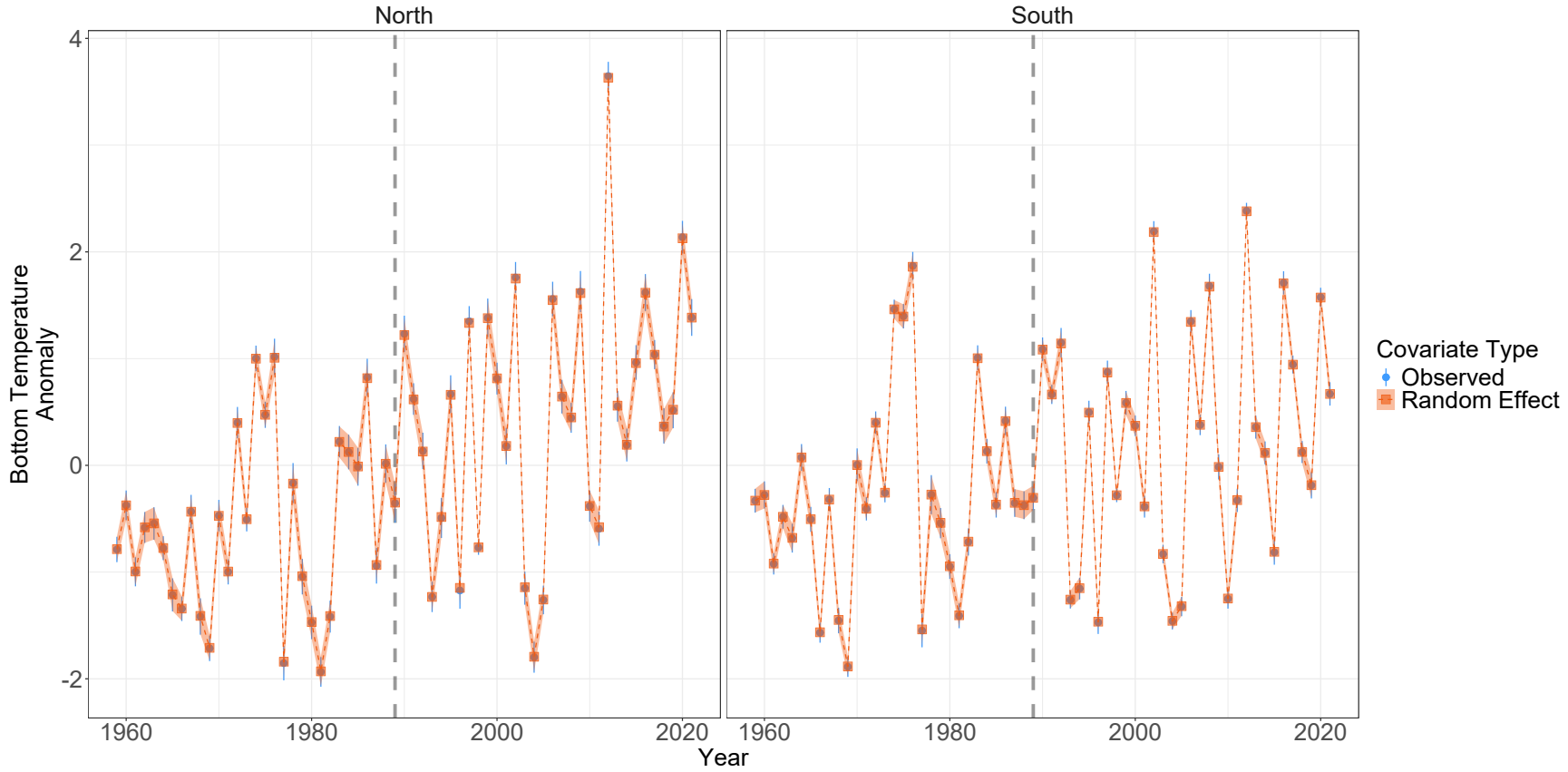

Figure S4: Observations with 95% confidence intervals (points with vertical lines) and posterior estimates with 95% confidence intervals (lines with polygons) of bottom temperature anomalies in the north and south regions from model M_1. Gray vertical line defines the first year that the black sea bass stock is modeled.

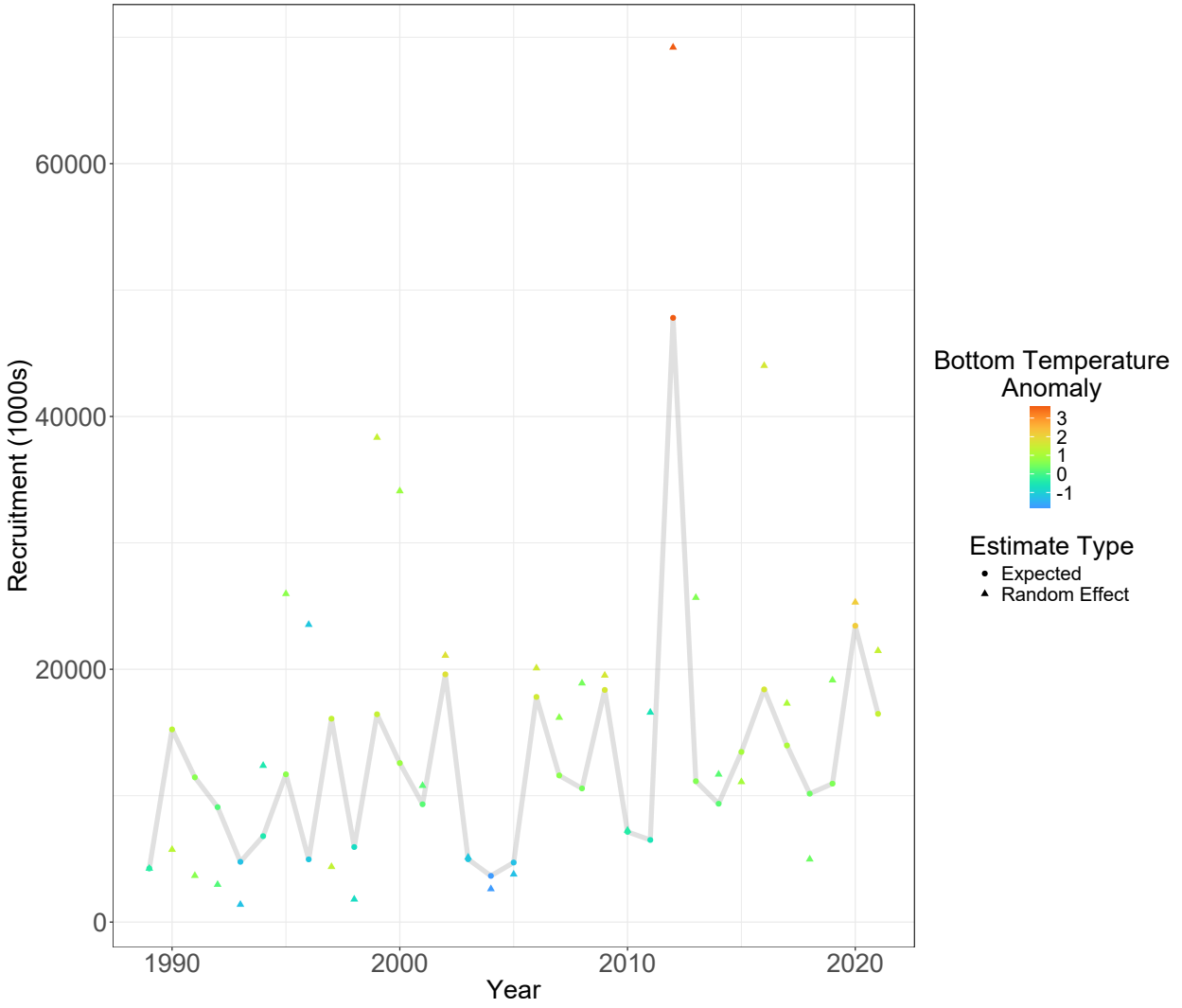

Figure S5: Expected and random effect recruitment estimates for the northern stock component. Color of points defined by the corresponding annual bottom temperature anomaly.

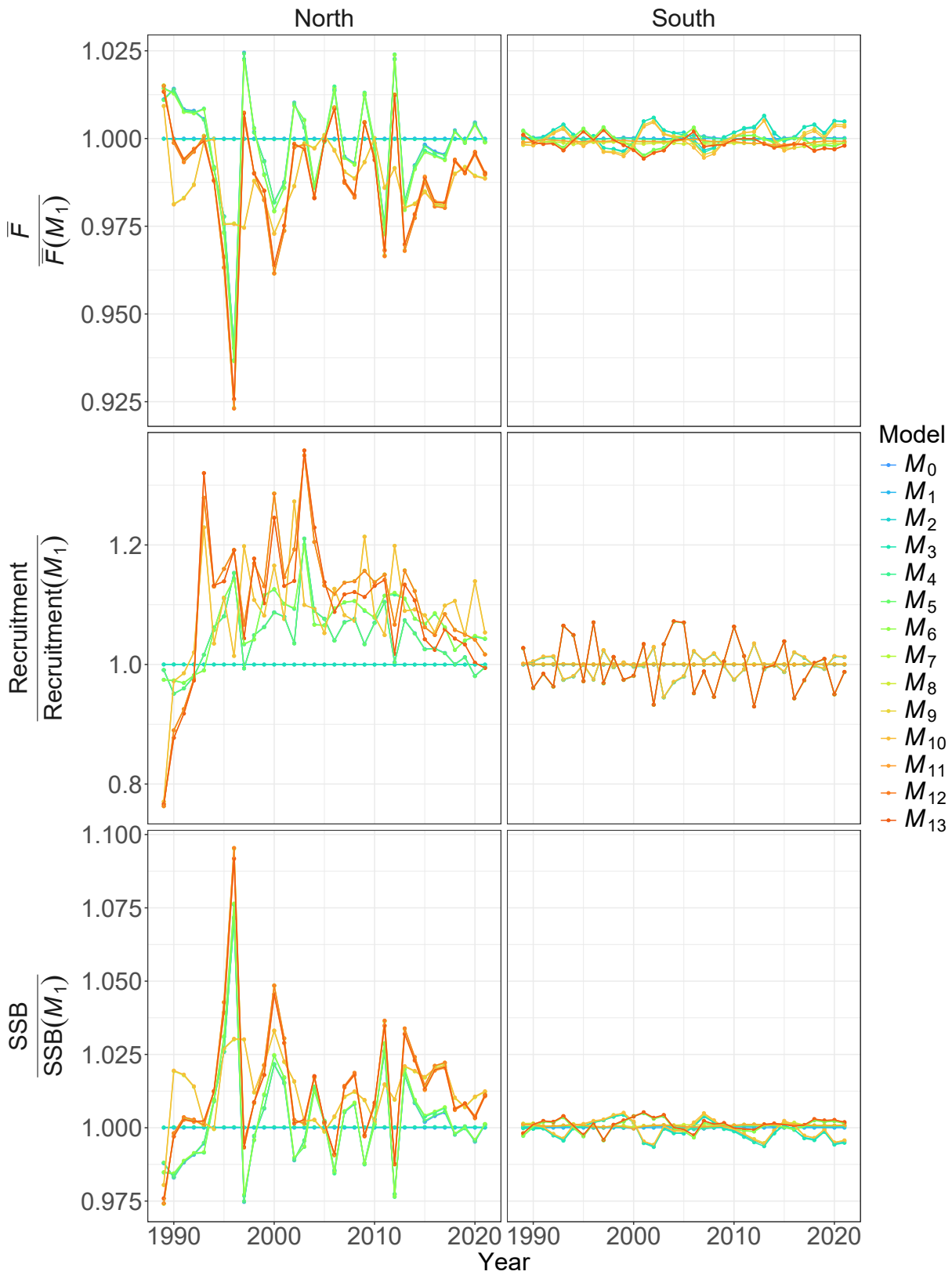

Figure S6: Estimates of SSB, F, and recruitment relative to those of the best performing model, M_1.

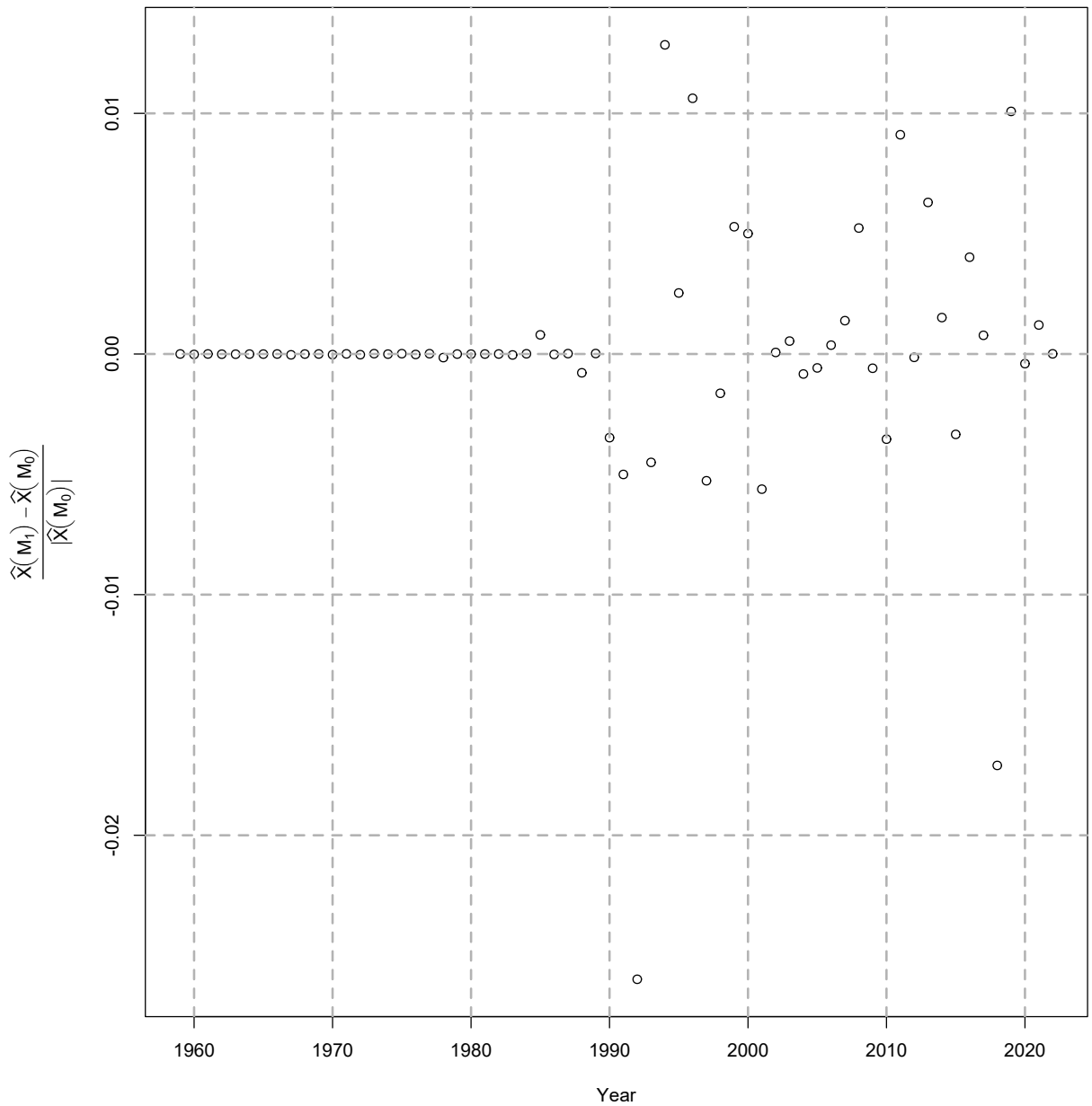

Figure S7: Relative differences in posterior estimates of northern region bottom temperature anomalies ($\widehat{X}$) from the null model without effects on recruitment (M_0) and with effects on the northern stock component (M_1).

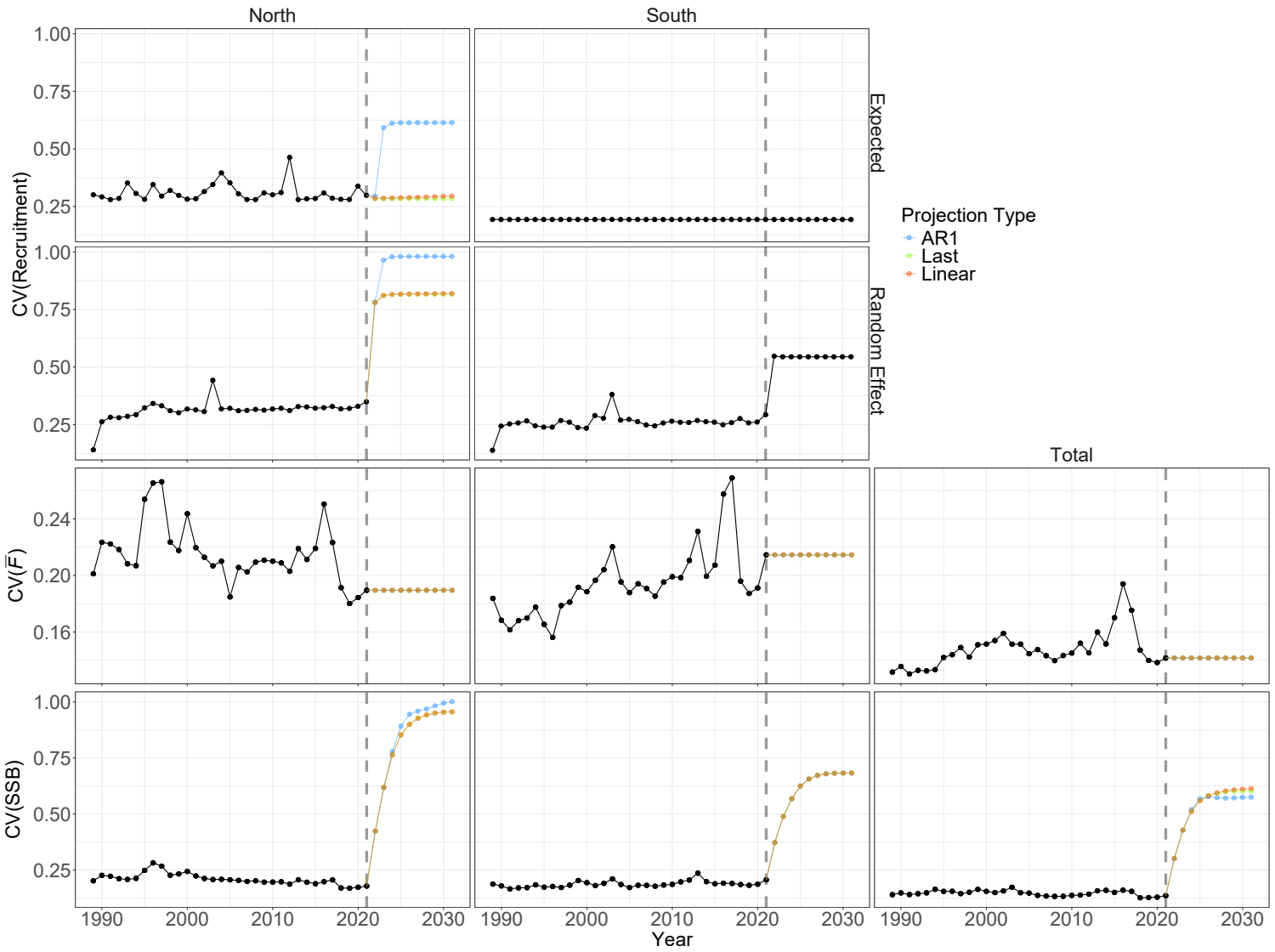

Figure S8: Coefficients of variation for estimates of alternative recruitment estimates (random effects or expected), average fishing mortality at age 6 and 7, and SSB by region and in total from model M_1. Values in years after 2021 are from projecting model M_1 under three alternative assumptions for the bottom temperature anomolies.

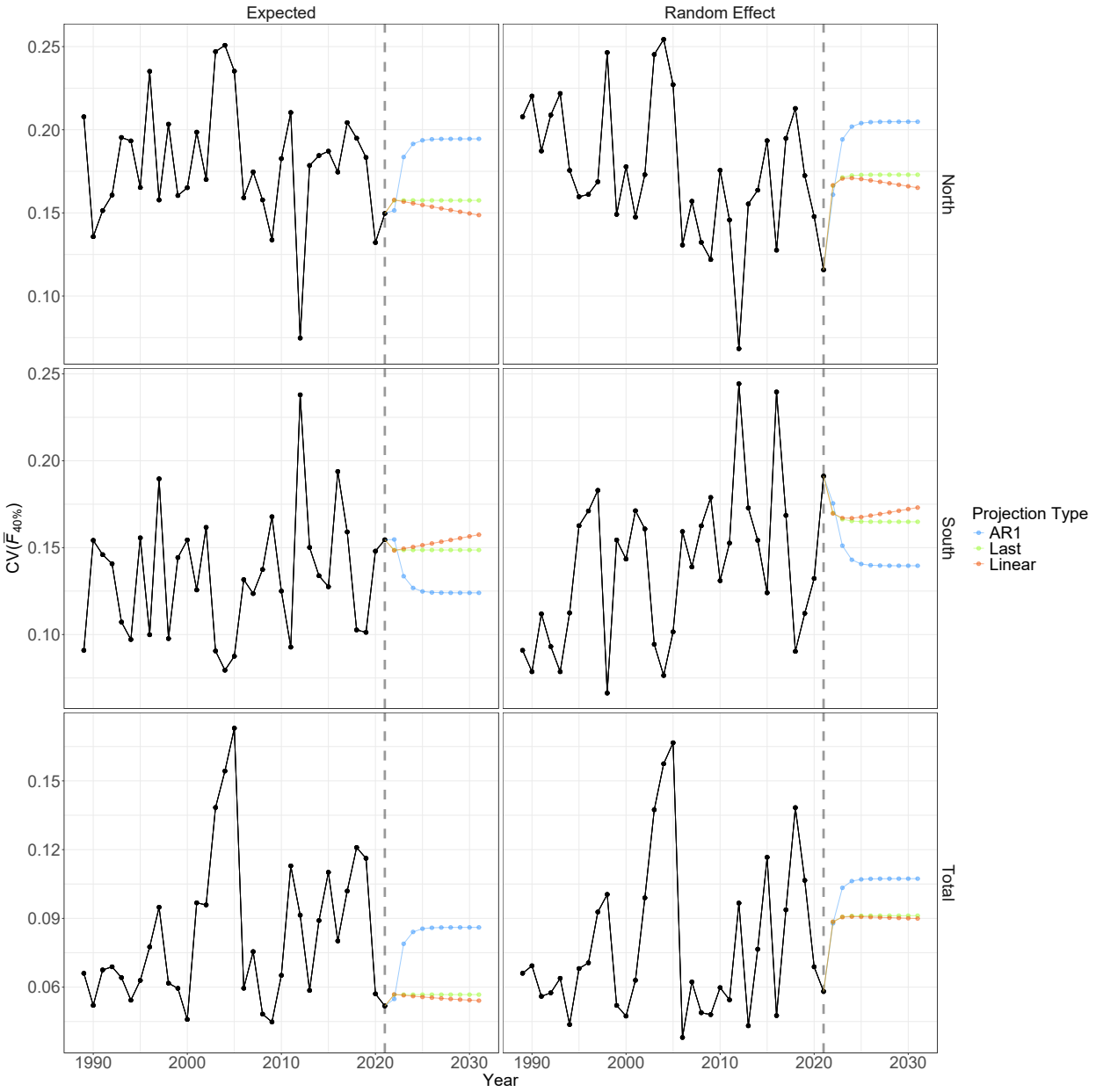

Figure S9: Coefficients of variation for annual equilibrium average F at ages 6 and 7 that produces the 40% spawning potential ratio as a function of annual expected recruitment or recruitment random effects and annual inputs to SSB/R calculations. Estimates in years after 2021 are from projecting model M_1 under three alternative assumptions for the bottom temperature anomolies.

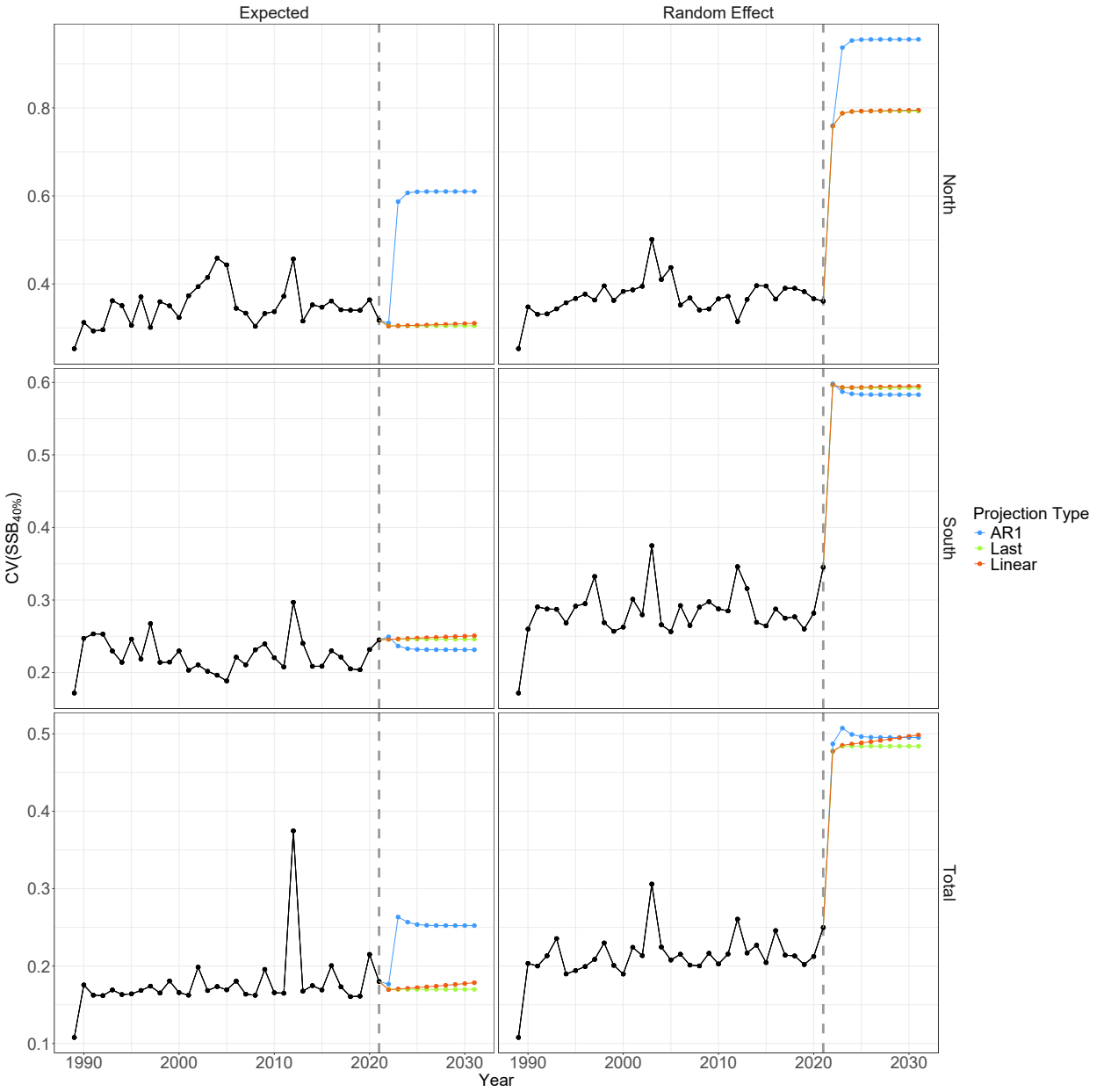

Figure S10: Coefficients of variation for annual equilibrium $SSB_{40\%}$ as a function of annual expected recruitment or recruitment random effects and annual inputs to SSB/R calculations and alternative annual recruitment types. Estimates in years after 2021 are from projecting model M_1 under three alternative assumptions for the bottom temperature anomolies.

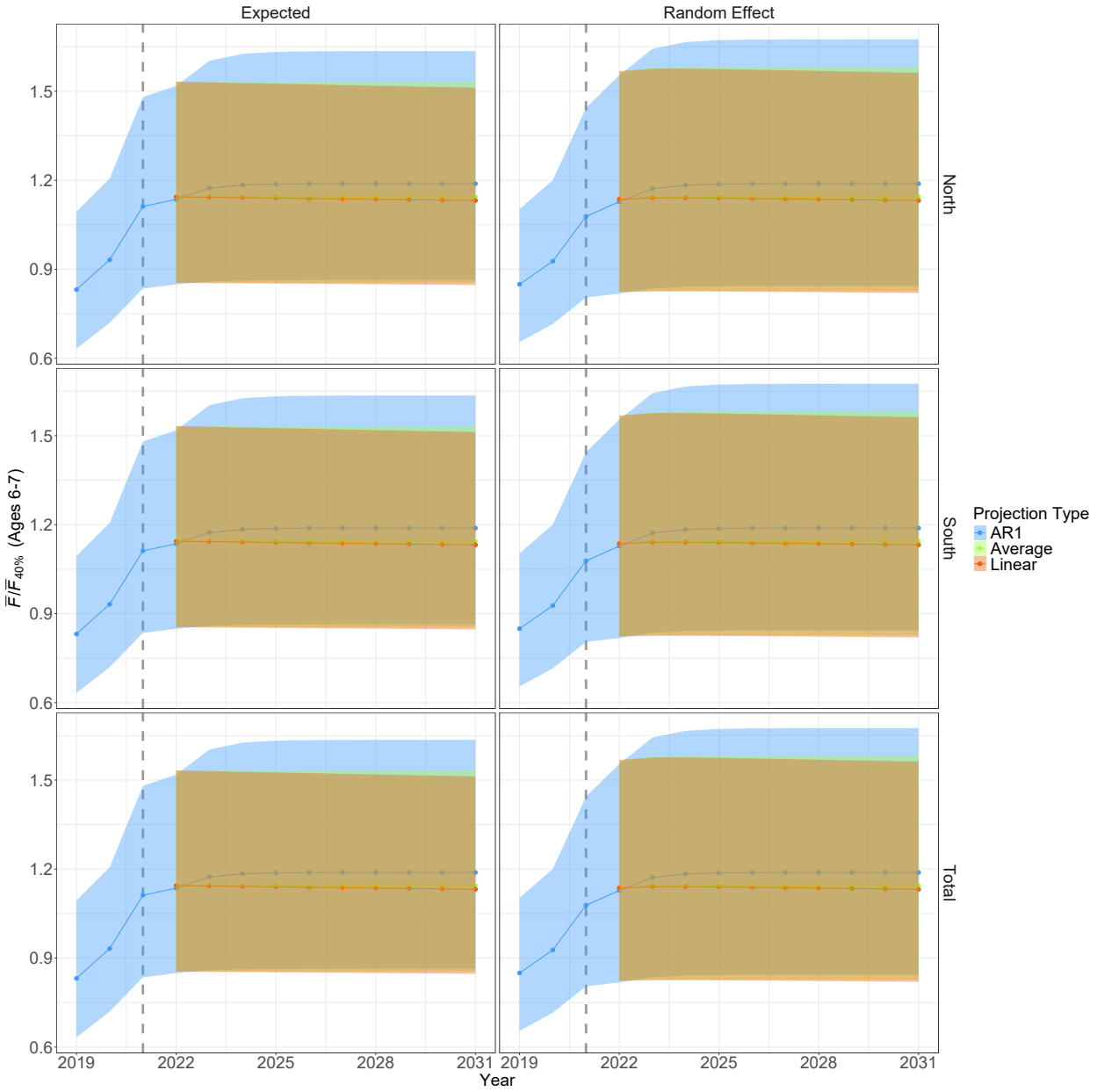

Figure S11: Annual estimates of ratios of fishing mortality to $F_{40\%}$ by region and in total. Estimates in years beyond 2021 are from projecting model M_1 under alternative assumptions for bottom temperature anomalies in the northern region. Vertical dotted line is the last year of data and polygons represent 95% confidence intervals.

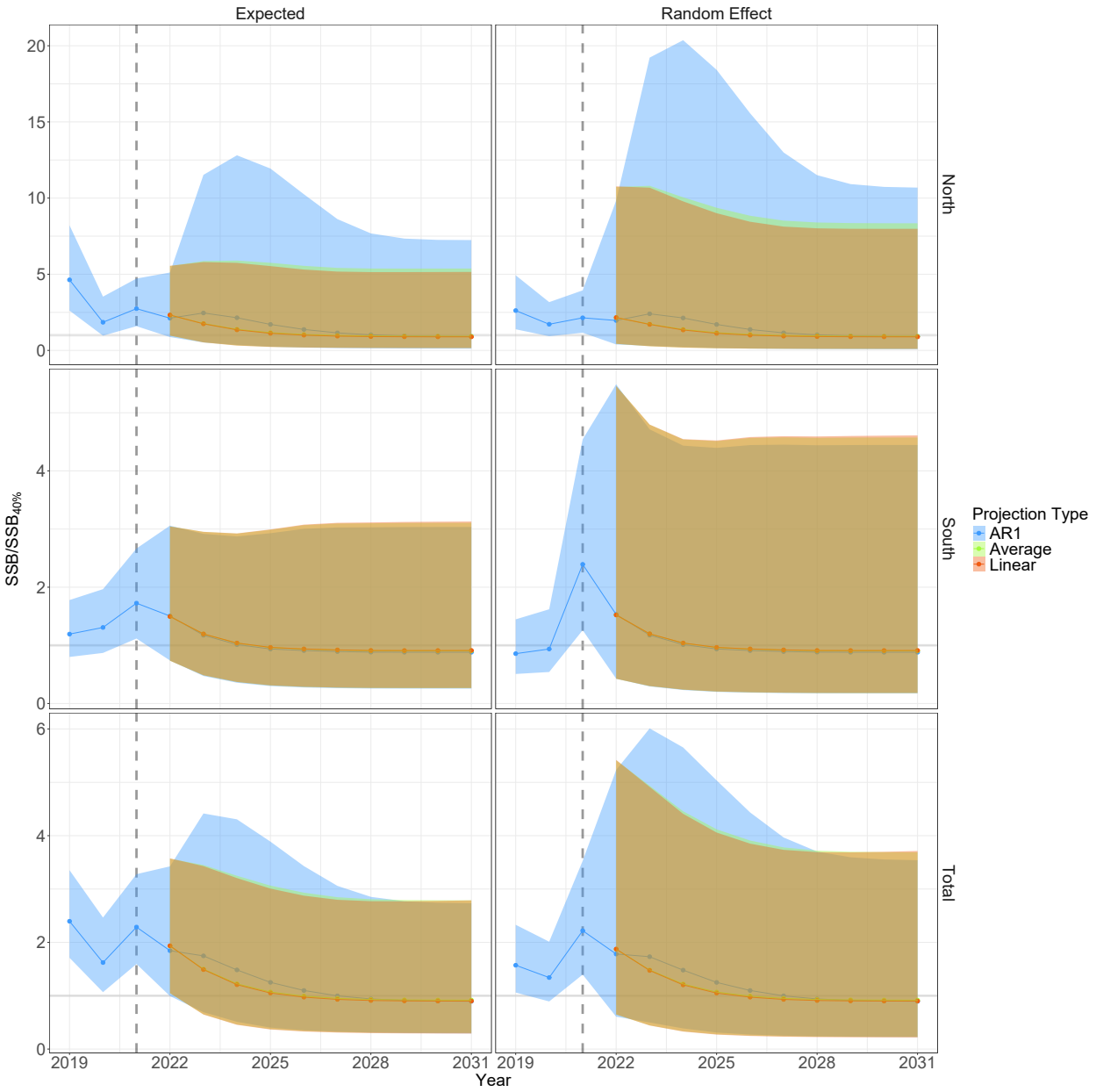

Figure S12: Annual estimates of ratios of SSB to $SSB_{40\%}$ by region and in total. Estimates in years beyond 2021 are from projecting model M_1 under alternative assumptions for bottom temperature anomalies in the northern region. Vertical dotted line is the last year of data and polygons represent 95% confidence intervals.

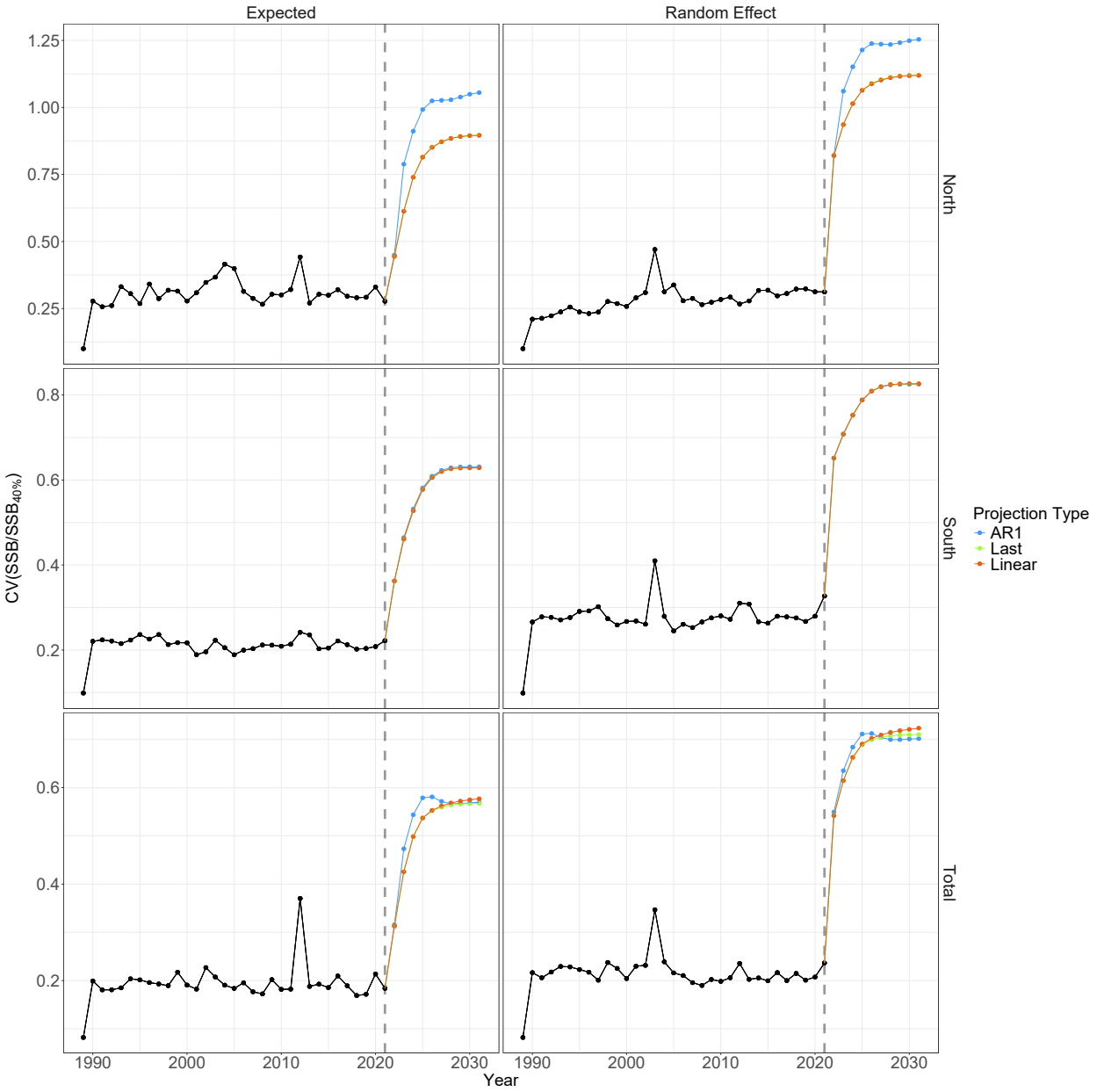

Figure S13: Coefficients of variation for annual ratios of SSB and equilibrium $SSB_{40\%}$ where the latter is a function of annual expected recruitment or recruitment random effects and annual inputs to SSB/R calculations. Estimates in years after 2021 are from projecting model M_1 under three alternative assumptions for the bottom temperature anomolies.

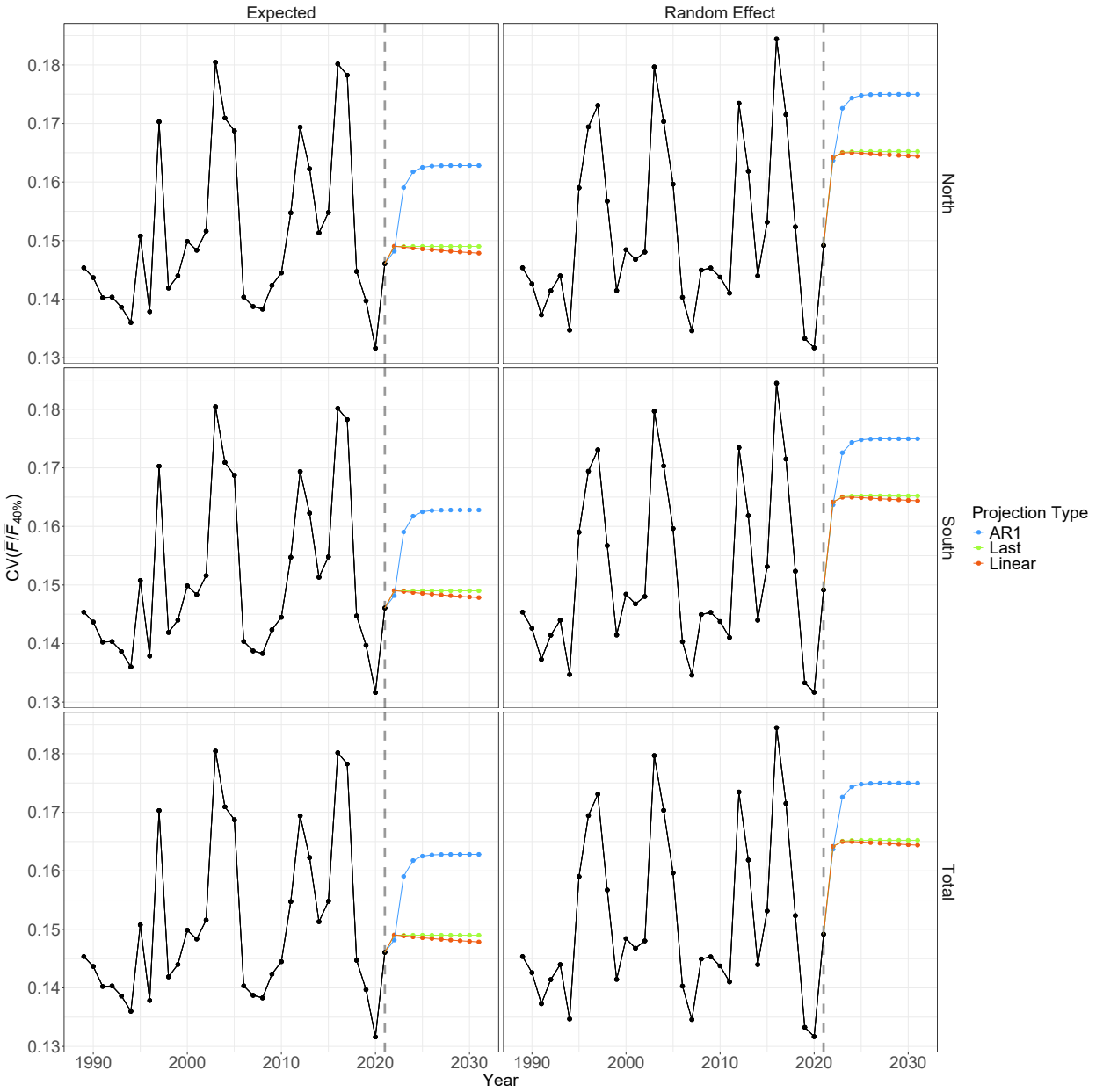

Figure S14: Coefficients of variation for annual ratios of average fishing mortality and equilibrium $\bar{F}_{40\%}$ at ages 6 and 7 where the latter is a function of annual expected recruitment or recruitment random effects and annual inputs to SSB/R calculations. Estimates in years after 2021 are from projecting model M_1 under three alternative assumptions for the bottom temperature anomolies.